Mixed Discontinuous Galerkin Approximation of the Maxwell Operator: Non-Stabilized Formulation

Paul Houston (paul.houston@mcs.le.ac.uk) *
Department of Mathematics and Computer Science, University of Leicester, Leicester LE1 7RH, UK

Ilaria Perugia (perugia@dimat.unipv.it)
Dipartimento di Matematica, Università di Pavia, Via Ferrata 1, 27100 Pavia, Italy

Dominik Schötzau (schotzau@math.unibas.ch) †
Department of Mathematics, University of Basel, Rheinsprung 21, 4051 Basel, Switzerland

Abstract. A non-stabilized mixed discontinuous Galerkin method for the discretization of the time-harmonic Maxwell operator on simplicial meshes is studied. In contrast to the stabilized scheme introduced in [8], the proposed formulation contains no normal–jump stabilization; instead, it is based on discontinuous mixed-order $(\mathbb{P}^\ell)^3 - \mathbb{P}^{\ell+1}$ elements for the approximation of the unknowns. A priori error bounds in the energy norm are derived that show convergence rates of the order $\mathcal{O}(h^\ell)$ in the mesh size h. The error analysis relies on suitable decompositions of discontinuous spaces and on stability properties of the underlying conforming spaces. The formulation is tested on a set of numerical examples in two space dimensions.

Keywords: Discontinuous Galerkin methods, Mixed methods, Maxwell operator

1. Introduction

In this paper, we propose, analyze and numerically test a non-stabilized mixed discontinuous Galerkin (DG) method on simplicial meshes for the numerical approximation of the time-harmonic Maxwell equations in the mixed form

$$\begin{aligned} \nabla \times (\mu^{-1}\nabla \times \mathbf{u}) - \varepsilon\nabla p &= \mathbf{j} \quad \text{in } \Omega, && (1a)\\ \nabla \cdot (\varepsilon\mathbf{u}) &= 0 \quad \text{in } \Omega, && (1b)\\ \mathbf{n}\times\mathbf{u} &= \mathbf{0} \quad \text{on } \Gamma, && (1c)\\ p &= 0 \quad \text{on } \Gamma. && (1d) \end{aligned}$$

Here, Ω is a bounded and simply-connected Lipschitz polyhedron in $\mathbb{R}^3$, $\Gamma = \partial\Omega$ its boundary, which we assume to be connected, and $\mathbf{n}$ the outward normal unit vector to Γ. The unknowns are the electric field $\mathbf{u}$, and

* Funded by the EPSRC (Grant GR/R76615).
† Partially supported by the Swiss NSF (Project 21-068126.02).

the Lagrange multiplier p related to the divergence free constraint; see, e.g., [5, 17]. The coefficients $\mu = \mu(\mathbf{x})$ and $\varepsilon = \varepsilon(\mathbf{x})$ are the magnetic permeability and the electric permittivity of the medium, respectively; they are assumed to be real functions which satisfy

$$0 < \mu_* \leq \mu(\mathbf{x}) \leq \mu^* < \infty, \quad 0 < \varepsilon_* \leq \varepsilon(\mathbf{x}) \leq \varepsilon^* < \infty, \quad \text{a.e. } \mathbf{x} \in \overline{\Omega}. \quad (2)$$

For simplicity, we further assume that μ and ε are piecewise constant with respect to a partition of the domain Ω into Lipschitz polyhedra. The right-hand side $\mathbf{j} \in L^2(\Omega)^3$ is an external source field.

This paper is a continuation of a series of papers, [15], [9], [16], and [8], devoted to the study of discontinuous Galerkin methods applied to the time-harmonic Maxwell equations. This study was initiated in [15] where an *hp*-local discontinuous Galerkin method was presented for the low-frequency approximation of the time-harmonic Maxwell equations in heterogeneous media. The focus there, however, was on the problem of how to discretize the curl-curl operator using discontinuous finite element spaces. The numerical experiments presented in [9] have confirmed the expected *hp*-convergence rates for smooth solutions, and indicate that DG methods can indeed be effective in a wide range of low-frequency applications with coercive bilinear forms. Later, in [16], a mixed discontinuous Galerkin formulation was presented to solve the high-frequency time-harmonic Maxwell equations in mixed form, where the underlying elliptic operator is of the form (1). The mixed form of the equations was chosen to provide control on the divergence of the electric field. For smooth material coefficients, optimal convergence of the method was proved by employing a duality approach, provided that appropriate *stabilization* terms were included in the formulation. From a practical point of view, these stabilization terms are very undesirable, as they tend to over–constrain the DG method, and may lead to large dispersion errors for problems with strong singularities. Subsequent work has shown that most of the stabilization terms employed in [16] are unnecessary; indeed, the amount of numerical stabilization has been drastically reduced in the formulation presented in the succeeding work [8]. Apart from the standard interior penalty terms, a *normal-jump* stabilization term is sufficient to render the mixed method in [8] well-posed for problem (1); this stabilization is easily achieved by a suitable (and locally conservative) choice of the numerical fluxes. The unknowns $\mathbf{u}$ and p are then approximated by discontinuous equal-order $(\mathbb{P}^\ell)^3 - \mathbb{P}^\ell$ elements on tetrahedral meshes, or by $(\mathbb{Q}^\ell)^3 - \mathbb{Q}^\ell$ elements on hexahedral meshes. This choice results in a mixed DG method that is optimally convergent in the DG-energy norm, with convergence rates of the order $\mathcal{O}(h^\ell)$ in the mesh size h. However, while this has been confirmed in practice, numerical experiments have also indicated that, on conforming meshes, the L^2–norm of the error in the approximation to $\mathbf{u}$ is sub-optimal by a full power of the mesh size.

In this paper, we study a *non-stabilized* variant of the approach in [8] on simplicial meshes, that was recently presented in [7]. In this context, the notion "non-stabilized" refers to the normal-jump stabilization. Indeed, we show that such stabilization terms are not necessary if mixed-order $(\mathbb{P}^\ell)^3 - \mathbb{P}^{\ell+1}$ elements are employed for the approximation of $\mathbf{u}$ and p. In fact, these elements can be viewed as a discontinuous version of the conforming pairing that is given by using Nédélec elements of the second type for the approximation of $\mathbf{u}$, and standard nodal $\mathbb{P}^{\ell+1}$ elements for p; see [14, 11]. The key advantages of this approach are that, firstly no additional stabilization is necessary to ensure that the underlying discretization is well–posed and optimally accurate in the DG energy norm. Secondly, although this new method leads to an increase in the number of degrees of freedom employed for the numerical approximation of the variable p, in comparison to the equal–order stabilized method introduced in [8], numerical experiments presented in Section 7 indicate that the L^2–norm of the error in the approximation to $\mathbf{u}$ is now fully optimal. Thereby, given that p is only a scalar variable, this increase in complexity is relatively small given that the order of approximation is increased by a full power of the mesh size for each component of the approximation to the *vector* variable $\mathbf{u}$.

The numerical analysis of the non-stabilized method proposed in this paper intrinsically differs from that in [8] for stabilized schemes, although the main result is essentially the same. Let us point out some of the main differences: in [8], the crucial stability result that gives coercivity of the discrete curl-curl form on a suitable kernel is obtained by using a duality approach. The control of all the terms then essentially relies on the normal-jump stabilization. This is no longer possible for the non-stabilized $(\mathbb{P}^\ell)^3 - \mathbb{P}^{\ell+1}$ method considered here. Instead, we use an *orthogonal decomposition* of the discontinuous finite element space $\mathbf{V}_h$ for the approximation of $\mathbf{u}$ into a direct sum of the form

$$\mathbf{V}_h = \mathbf{V}_h^c \oplus \mathbf{V}_h^\perp,$$

where $\mathbf{V}_h^c$ is the *$H($*curl*$)$-conforming* Nédélec finite element space of the second type (see [14]), and $\mathbf{V}_h^\perp$ is a suitable orthogonal complement. We then make use of well-known stability results for conforming elements to control error contributions in $\mathbf{V}_h^c$, and employ the interior penalty terms present in our formulation to control those in $\mathbf{V}_h^\perp$. This approach is very much in the spirit of the recent techniques developed in [4] for the analysis of stabilized finite element methods. To control the non-conformity of the method in the Lagrange multiplier p, we use a similar decomposition of the related discrete space Q_h, namely, $Q_h = Q_h^c \oplus$

$Q_h^\perp$, where Q_h^c is a standard H^1-conforming finite element space; this decomposition of Q_h was also employed in [8]. Then, at the heart of our analysis are norm-equivalence properties for the above decompositions of discontinuous spaces which might be of interest on their own.

Finally, we point out that the techniques in this paper can be used almost verbatim to analyze the well-posedness and convergence of the analogous mixed DG method that is obtained by using discontinuous Nédélec elements of the first type for the approximation of $\mathbf{u}$ (see [12, 13, 11]), and discontinuous $\mathbb{P}^\ell$ elements for p; see also Remark 2 below. This family can be easily extended to hexahedral meshes whereas the discontinuous $(\mathbb{P}^\ell)^3 - \mathbb{P}^{\ell+1}$ pairing proposed in this paper does not seem to have a natural extension to hexahedra; we note that this is also the case for its conforming counterpart.

The outline of the paper is as follows. We begin by detailing the notation for the function spaces that we use throughout the paper. In Section 2, we present the non-stabilized mixed discontinuous Galerkin approximation for (1) on tetrahedral meshes. In Section 3, we state our main results, namely, optimal a priori error estimates for the approximate solution. Section 4 is concerned with a decomposition result that is instrumental in our analysis; this proof is postponed to the appendix. In Section 5, we introduce an auxiliary mixed formulation and discuss the stability properties of the forms involved. Then, the error bounds are proved in Section 6. Finally, in Section 7, we test the performance of the proposed method on a series of numerical experiments. The presentation is ended with concluding remarks in Section 8.

Notation. Given a bounded domain D in $\mathbb{R}^2$ or $\mathbb{R}^3$, we denote by $H^s(D)$ the standard Sobolev space of functions with regularity exponent $s \geq 0$, and norm $\|\cdot\|_{s,D}$. For $t = 0$, we write $L^2(D)$ in lieu of $H^0(D)$. We also write $\|\cdot\|_{s,D}$ to denote the norm for the space $H^s(D)^d$, $d = 2, 3$. Given $D \subset \mathbb{R}^3$, $H(\text{curl}; D)$ is the space of vector field $\mathbf{u} \in L^2(D)^3$ with $\nabla \times \mathbf{u} \in L^2(D)^3$, endowed with the corresponding graph norm. We denote by $H_0^1(D)$ and $H_0(\text{curl}; D)$ the subspaces of $H^1(D)$ and $H(\text{curl}; D)$ of functions with zero trace and zero tangential trace, respectively.

2. Non-stabilized mixed DG discretization

In this section we introduce a non-stabilized mixed discontinuous Galerkin discretization of problem (1).

2.1. Variational formulation

Set $\mathbf{V} = H_0(\mathrm{curl};\Omega)$ and $Q = H_0^1(\Omega)$. The standard variational form of problem (1) consists in finding $(\mathbf{u}, p) \in \mathbf{V} \times Q$ such that

$$\begin{aligned} a(\mathbf{u},\mathbf{v}) \;+\; b(\mathbf{v},p) &= \textstyle\int_\Omega \mathbf{j}\cdot\mathbf{v}\,d\mathbf{x},\\ b(\mathbf{u},q) &= 0 \end{aligned}$$

for all $(\mathbf{v}, q) \in \mathbf{V}\times Q$, where the forms a and b are defined, respectively, by

$$\begin{aligned} a(\mathbf{u},\mathbf{v}) &= \int_\Omega \mu^{-1}\nabla\times\mathbf{u}\cdot\nabla\times\mathbf{v}\,d\mathbf{x},\\ b(\mathbf{v},p) &= -\int_\Omega \varepsilon\mathbf{v}\cdot\nabla p\,d\mathbf{x}. \end{aligned}$$

Well-posedness of the above formulation follows from the standard theory of mixed problems [3], since a is bilinear, continuous and coercive on the kernel of b, and b is linear and continuous, and satisfies the inf-sup condition; see, e.g., [5, 17] for details.

2.2. Meshes, finite element spaces and traces

Throughout, we consider shape-regular conforming meshes $\mathcal{T}_h$ that partition the domain Ω into tetrahedra; we always assume that the meshes are aligned with the discontinuities in the coefficients μ and ε. Each element is affinely equivalent to the reference tetrahedron $\widehat{K} = \{\hat{x}_1, \hat{x}_2, \hat{x}_3 > 0 : \hat{x}_1 + \hat{x}_2 + \hat{x}_3 < 1\}$. We denote by $\mathcal{F}_h^{\mathcal{I}}$ the set of all interior faces of $\mathcal{T}_h$, by $\mathcal{F}_h^{\mathcal{B}}$ the set of all boundary faces of $\mathcal{T}_h$, and set $\mathcal{F}_h = \mathcal{F}_h^{\mathcal{I}} \cup \mathcal{F}_h^{\mathcal{B}}$. Similarly, $\mathcal{E}_h^{\mathcal{I}}$ denotes the set of interior edges, $\mathcal{E}_h^{\mathcal{B}}$ the set of boundary edges, and $\mathcal{E}_h = \mathcal{E}_h^{\mathcal{I}} \cup \mathcal{E}_h^{\mathcal{B}}$.

For an element $K \in \mathcal{T}_h$, we denote by $\mathbb{P}^\ell(K)$ the space of polynomials of total degree at most ℓ, $\ell \geq 0$, on K. The generic discontinuous finite element space of piecewise polynomials is given by

$$P^\ell(\mathcal{T}_h) = \{u \in L^2(\Omega) : u|_K \in \mathbb{P}^\ell(K) \;\; \forall K \in \mathcal{T}_h\}.$$

For piecewise smooth vector- and scalar-valued functions $\mathbf{v}$ and q, we introduce the following trace operators. Let $f \in \mathcal{F}_h^{\mathcal{I}}$ be an interior face shared by two elements K^+ and K^-, and write $\mathbf{n}^\pm$ for the outward normal unit vectors to the boundaries $\partial K^\pm$, respectively. Denoting by $\mathbf{v}^\pm$ and $q^\pm$ the traces of $\mathbf{v}$ and q on $\partial K^\pm$ taken from within $K^\pm$, respectively, we define the *jumps* across f by

$$[\![\mathbf{v}]\!]_T = \mathbf{n}^+\times\mathbf{v}^+ + \mathbf{n}^-\times\mathbf{v}^-, \qquad [\![q]\!]_N = q^+\mathbf{n}^+ + q^-\mathbf{n}^-,$$

and the *averages* by $\{\!\{\mathbf{v}\}\!\} = (\mathbf{v}^+ + \mathbf{v}^-)/2$ and $\{\!\{q\}\!\} = (q^+ + q^-)/2$. On a boundary face $f \in \mathcal{F}_h^{\mathcal{B}}$, we set $[\![\mathbf{v}]\!]_T = \mathbf{n} \times \mathbf{v}$, $[\![q]\!]_N = q\,\mathbf{n}$, $\{\!\{\mathbf{v}\}\!\} = \mathbf{v}$ and $\{\!\{q\}\!\} = q$.

2.3. Discontinuous Galerkin discretization

For a given partition $\mathcal{T}_h$ of Ω, and an approximation order $\ell \geq 1$, we define the following finite element spaces:

$$\mathbf{V}_h = P^{\ell}(\mathcal{T}_h)^3, \qquad Q_h = P^{\ell+1}(\mathcal{T}_h). \tag{3}$$

With this notation, we consider the following discontinuous Galerkin method: find $(\mathbf{u}_h, p_h)$ in $\mathbf{V}_h \times Q_h$ such that

$$a_h(\mathbf{u}_h, \mathbf{v}) + b_h(\mathbf{v}, p_h) = \textstyle\int_\Omega \mathbf{j} \cdot \mathbf{v}\, d\mathbf{x}, \tag{4a}$$

$$b_h(\mathbf{u}_h, q) - c_h(p_h, q) = 0 \tag{4b}$$

for all $(\mathbf{v}, q) \in \mathbf{V}_h \times Q_h$, where the discrete forms a_h, b_h and c_h are defined, respectively, by

$$\begin{aligned} a_h(\mathbf{u},\mathbf{v}) &= \int_\Omega \mu^{-1}\nabla_h \times \mathbf{u} \cdot \nabla_h \times \mathbf{v}\, d\mathbf{x} - \int_{\mathcal{F}_h} [\![\mathbf{u}]\!]_T \cdot \{\!\{\mu^{-1}\nabla_h \times \mathbf{v}\}\!\}\, ds \\ &\quad - \int_{\mathcal{F}_h} [\![\mathbf{v}]\!]_T \cdot \{\!\{\mu^{-1}\nabla_h \times \mathbf{u}\}\!\}\, ds + \int_{\mathcal{F}_h} \mathsf{a}\, [\![\mathbf{u}]\!]_T \cdot [\![\mathbf{v}]\!]_T\, ds, \\ b_h(\mathbf{v},p) &= -\int_\Omega \varepsilon\mathbf{v} \cdot \nabla_h p\, d\mathbf{x} + \int_{\mathcal{F}_h} \{\!\{\varepsilon\mathbf{v}\}\!\} \cdot [\![p]\!]_N\, ds, \\ c_h(p,q) &= \int_{\mathcal{F}_h} \mathsf{c}[\![p]\!]_N \cdot [\![q]\!]_N\, ds. \end{aligned}$$

Here, $\nabla_h\times$ and ∇_h denote the elementwise curl and gradient operators, respectively. Further, we have set $\int_{\mathcal{F}_h} \varphi(s)\, ds = \sum_{f\in\mathcal{F}_h} \int_f \varphi(s)\, ds$.

The form a_h corresponds to the interior penalty discretization of the curl-curl operator [9, 16, 8]; notice that, unlike in [8], no normal-jump stabilization has been introduced into this form. This is the reason why we refer to (4) as a *non-stabilized formulation.* The form b_h discretizes the divergence operator in a DG fashion, and the form c_h is the interior penalty form that weakly enforces the continuity of p_h. The parameters a and c are the usual *interior penalty* parameters that will be chosen later on, depending on the mesh size and the coefficients μ and ε.

REMARK 1. *For inhomogeneous boundary conditions $\mathbf{n}\times\mathbf{u} = \mathbf{g}$ on Γ, where the datum $\mathbf{g}$ is a prescribed tangential trace belonging to $L^2(\Gamma)^3$, the right-hand side in (4a) has to be replaced by the functional f_h given by*

$$f_h(\mathbf{v}) = \int_\Omega \mathbf{j}\cdot\mathbf{v}\, d\mathbf{x} - \int_{\mathcal{F}_h^{\mathcal{B}}} \mathbf{g}\cdot\mu^{-1}\nabla_h \times \mathbf{v}\, ds + \int_{\mathcal{F}_h^{\mathcal{B}}} \mathsf{a}\,\mathbf{g}\cdot(\mathbf{n}\times\mathbf{v})\, ds.$$

Here, the integral over $\mathcal{F}_h^{\mathcal{B}}$ is understood as the sum of the integrals over all the boundary faces.

3. Main results

In this section, we consider the well–posedness and a priori error analysis of the mixed DG method (4).

3.1. Interior penalty parameters, DG-spaces and norms

In order to define the interior penalty parameters $\mathtt{a}$ and $\mathtt{c}$ arising in the mixed DG method (4), we first need to introduce some notation. To this end, we write h_K to denote the diameter of element $K \in \mathcal{T}_h$; the mesh size is then given by $h = \max_{K\in\mathcal{T}_h} h_K$. On the faces in $\mathcal{F}_h$, we define the function $\mathtt{h}$ by

$$\mathtt{h}(\mathbf{x}) = \begin{cases} \min\{h_K, h_{K'}\} & \text{if } \mathbf{x} \text{ is in the interior of } \partial K \cap \partial K', \\ h_K & \text{if } \mathbf{x} \text{ is in the interior of } \partial K \cap \Gamma. \end{cases}$$

Similarly, we define the functions $\mathtt{m}$ and $\mathtt{e}$ by $\mathtt{m}(\mathbf{x}) = \min\{\mu_K, \mu_{K'}\}$ and $\mathtt{e}(\mathbf{x}) = \max\{\varepsilon_K, \varepsilon_{K'}\}$, if $\mathbf{x}$ is in the interior of $\partial K \cap \partial K'$, and $\mathtt{m}(\mathbf{x}) = \mu_K$ and $\mathtt{e}(\mathbf{x}) = \varepsilon_K$, if $\mathbf{x}$ is in the interior of $\partial K \cap \Gamma$, with μ_K and ε_K denoting the restrictions of μ and ε, respectively, to the element K (recall that μ and ε are constant within each element). We then choose the interior penalty functions $\mathtt{a}$ and $\mathtt{c}$ as follows:

$$\mathtt{a} = \alpha\, \mathtt{m}^{-1}\mathtt{h}^{-1}, \qquad \mathtt{c} = \gamma\, \mathtt{e}\mathtt{h}^{-1}, \tag{5}$$

where α and γ are positive parameters independent of the mesh size and the coefficients μ and ε.

We define the spaces

$$\mathbf{V}(h) = \mathbf{V} + \mathbf{V}_h, \qquad Q(h) = Q + Q_h,$$

endowed with the following seminorm and norms, respectively:

$$\begin{aligned} |\mathbf{v}|^2_{\mathbf{V}(h)} &= \|\mu^{-\frac{1}{2}} \nabla_h \times \mathbf{v}\|^2_{0,\Omega} + \|\mathtt{m}^{-\frac{1}{2}}\mathtt{h}^{-\frac{1}{2}} [\![\mathbf{v}]\!]_T\|^2_{0,\mathcal{F}_h}, \\ \|\mathbf{v}\|^2_{\mathbf{V}(h)} &= \|\varepsilon^{\frac{1}{2}}\mathbf{v}\|^2_{0,\Omega} + |\mathbf{v}|^2_{\mathbf{V}(h)}, \\ \|q\|^2_{Q(h)} &= \|\varepsilon^{\frac{1}{2}}\nabla_h q\|^2_{0,\Omega} + \|\mathtt{e}^{\frac{1}{2}}\mathtt{h}^{-\frac{1}{2}}[\![q]\!]_N\|^2_{0,\mathcal{F}_h}. \end{aligned}$$

Here, we use the notation

$$\|\boldsymbol{\varphi}\|^2_{0,\mathcal{F}_h} := \sum_{f\in\mathcal{F}_h} \|\boldsymbol{\varphi}\|^2_{0,f}.$$

Finally, for $(\mathbf{v}, q)$ in $\mathbf{V}(h) \times Q(h)$, we introduce the DG-norm

$$|||(\mathbf{v}, q)|||_{\mathrm{DG}} = \|\mathbf{v}\|_{\mathbf{V}(h)} + \|q\|_{Q(h)}.$$

3.2. Well-posedness of the discrete problem

The following ellipticity property of the form a_h is essential for the proof of the well-posedness of the DG-discrete problem.

PROPOSITION 1. *There is a parameter $\alpha_0 > 0$ independent of the mesh size and the coefficients μ and ε such that for parameters α in (5) with $\alpha > \alpha_0$ we have that*

$$a_h(\mathbf{v}, \mathbf{v}) \geq C\, |\mathbf{v}|^2_{\mathbf{V}(h)}$$

for all $\mathbf{v} \in \mathbf{V}_h$, where C is a positive constant, independent of the mesh size and the coefficients μ and ε.

Proof. This result can be proved as in [2, 9, 16], taking into account the definition of $\mathtt{m}$. We note that the minimal value of α_0, which guarantees the ellipticity property only depends on the shape regularity of the mesh $\mathcal{T}_h$ and on the polynomial approximation degree ℓ. □

Let us now show the existence and uniqueness of solutions to formulation (4), provided that α is chosen sufficiently large.

PROPOSITION 2. *For parameters α and γ in (5) with $\alpha > \alpha_0$ and $\gamma > 0$, the mixed DG method (4) possesses a unique solution.*

Proof. Due to the linearity and finite-dimensionality of the problem, it is enough to show that $\mathbf{j} = \mathbf{0}$ implies $\mathbf{u}_h = \mathbf{0}$ and $p_h = 0$. To this end, we select $\mathbf{v} = \mathbf{u}_h$ in (4a) and $q = p_h$ in (4b), and subtract (4b) from (4a). From Proposition 1, it follows that $\nabla_h \times \mathbf{u}_h = \mathbf{0}$ on each element in $\mathcal{T}_h$, and that $[\![\mathbf{u}_h]\!]_T = \mathbf{0}$ and $[\![p_h]\!]_N = \mathbf{0}$ on each face in $\mathcal{F}_h$. Therefore, $p_h \in Q_h \cap H^1_0(\Omega)$ and $\mathbf{u}_h$ is a curl-free function belonging to the Nédélec finite element space of the second type, with zero tangential trace on Γ. This implies that $\mathbf{u}_h = \nabla \psi_h$, for some $\psi_h \in Q_h \cap H^1_0(\Omega)$ (see [14, Theorem 7] and [11, p. 209]). Then, equation (4b) implies that $\mathbf{u}_h$ is actually zero. Equation (4a) then becomes $\int_\Omega \varepsilon \mathbf{v} \cdot \nabla p_h \, d\mathbf{x} = 0$, for any $\mathbf{v} \in V_h$; thereby $\nabla p_h = \mathbf{0}$. Employing this result, together with $p_h = 0$ on Γ, we deduce that $p_h = 0$. □

From now on, we assume that $\alpha > \alpha_0$.

3.3. A priori error bound

The main result of this paper is stated in the following theorem.

THEOREM 1. *Given that the analytical solution* $(\mathbf{u}, p)$ *of (1) possesses the following Sobolev regularity:*

$$\varepsilon\mathbf{u} \in H^s(\Omega)^3, \quad \mu^{-1}\nabla\times\mathbf{u} \in H^s(\Omega)^3 \quad \text{and} \quad p \in H^{s+1}(\Omega), \tag{6}$$

for an exponent $s > 1/2$. *Then, the mixed DG approximation* $(\mathbf{u}_h, p_h)$ *defined by (4), with* $\alpha > \alpha_0$ *and* $\gamma > 0$, *satisfies the following a priori error bound*

$$\begin{aligned}&|||(\mathbf{u}-\mathbf{u}_h, p-p_h)|||_{\mathrm{DG}}\\ &\qquad\le C\,h^{\min\{s,\ell\}}\left[\|\varepsilon\mathbf{u}\|_{s,\Omega} + \|\mu^{-1}\nabla\times\mathbf{u}\|_{s,\Omega} + \|p\|_{s+1,\Omega}\right],\end{aligned}$$

where C *is a positive constant, depending on the bounds (2) on the coefficients* μ *and* ε, *the shape-regularity of the mesh, the interior penalty parameters* α *and* γ, *and the polynomial degree* ℓ, *but independent of the mesh size* h.

REMARK 2. *We note that the above theorem also holds when* $\mathbf{V}_h$ *is replaced by the discontinuous version of Nédélec's first family of finite elements, see [12, 13], and* $Q_h = P^\ell(\mathcal{T}_h)$. *While this space is less convenient in a discontinuous Galerkin setting as the elemental spaces are not full polynomial spaces, an analogous (discontinuous) pairing can also be constructed on hexahedral meshes. On the other hand, as for their conforming counterparts, the finite element spaces (3) do not have a natural extension to hexahedra.*

The next three sections are devoted to the proof of Theorem 1. We begin in Section 4 by establishing a crucial decomposition result for the discontinuous spaces. In Section 5, we introduce an auxiliary mixed formulation and discuss its stability properties. Finally, in Section 6, the detailed proof of the error bound in Theorem 1 is given.

4. Decomposition of the discontinuous spaces

In this section, we present an orthogonal decomposition of the spaces $\mathbf{V}_h$ and Q_h and state crucial norm-equivalence properties. These results allow us to employ the stability properties of the underlying conforming spaces.

To this end, we decompose $\mathbf{V}_h$ and Q_h into

$$\mathbf{V}_h = \mathbf{V}_h^c \oplus \mathbf{V}_h^\perp, \qquad Q_h = Q_h^c \oplus Q_h^\perp, \tag{7}$$

respectively. Here, $\mathbf{V}_h^c = \mathbf{V}_h \cap H_0(\mathrm{curl};\Omega)$ is the Nédélec finite element space of second type, with zero tangential trace prescribed on Γ, and

$\mathbf{V}_h^\perp$ is its $\mathbf{V}(h)$–orthogonal complement in $\mathbf{V}_h$. Similarly, $Q_h^c = Q_h \cap H_0^1(\Omega)$ is the space of continuous polynomials of degree $\ell+1$, with zero trace prescribed on Γ, and $Q_h^\perp$ is its $Q(h)$–orthogonal complement in Q_h. We observe that the expressions

$$\|\mathbf{v}\|_{\mathbf{V}_h^\perp} = \|\mathtt{m}^{-\frac{1}{2}}\mathbf{h}^{-\frac{1}{2}}[\![\mathbf{v}]\!]_T\|_{0,\mathcal{F}_h}, \qquad \|q\|_{Q_h^\perp} = \|\mathtt{e}^{\frac{1}{2}}\mathbf{h}^{-\frac{1}{2}}[\![p]\!]_N\|_{0,\mathcal{F}_h}$$

define norms on $\mathbf{V}_h^\perp$ and $Q_h^\perp$, respectively.

The following norm-equivalence result will form the basis of our analysis.

THEOREM 2. *There exist constants C_1 and C_2, independent of the mesh size h, such that*

$$C_1\|\mathbf{v}\|_{\mathbf{V}(h)} \leq \|\mathbf{v}\|_{\mathbf{V}_h^\perp} \leq \|\mathbf{v}\|_{\mathbf{V}(h)}, \tag{8}$$

$$C_2\|q\|_{Q(h)} \leq \|q\|_{Q_h^\perp} \leq \|q\|_{Q(h)}, \tag{9}$$

for any $\mathbf{v} \in \mathbf{V}_h^\perp$ and any $q \in Q_h^\perp$, respectively.

The equivalence property (9) was proved in [8]. Its proof relies on the same approximation result that was used in [10, Theorem 2.2 and Theorem 2.3] to derive a-posteriori error bounds for DG discretizations of diffusion problems. The proof of (8) can be developed along the same lines and will be carried out in the appendix.

5. Stability properties of an auxiliary formulation

For the purposes of the analysis, it is convenient to rewrite the discontinuous Galerkin method (4) in a non-consistent form, based on the introduction of lifting functions (see [2]). The stability properties of the forms arising in this auxiliary formulation will then be discussed.

5.1. Auxiliary mixed formulation

To rewrite the formulation (4) in a non-consistent form, for $\mathbf{v} \in \mathbf{V}(h)$, we define the lifted element $\mathcal{L}(\mathbf{v}) \in \mathbf{V}_h$ by

$$\int_\Omega \mathcal{L}(\mathbf{v}) \cdot \mathbf{w}\, d\mathbf{x} = \int_{\mathcal{F}_h} [\![\mathbf{v}]\!]_T \cdot \{\!\{\mathbf{w}\}\!\}\, ds \qquad \forall \mathbf{w} \in \mathbf{V}_h;$$

for q in $Q(h)$, we define $\mathcal{M}(q) \in \mathbf{V}_h$ by

$$\int_\Omega \mathcal{M}(q) \cdot \mathbf{w}\, d\mathbf{x} = \int_{\mathcal{F}_h} \{\!\{\mathbf{w}\}\!\} \cdot [\![q]\!]_N\, ds \qquad \forall \mathbf{w} \in \mathbf{V}_h.$$

Additionally, we introduce the perturbed forms

$$\begin{aligned}\widetilde{a}_h(\mathbf{u},\mathbf{v}) &= \int_\Omega \mu^{-1}\nabla_h\times\mathbf{u}\cdot\nabla_h\times\mathbf{v}\,d\mathbf{x} - \int_\Omega \mathcal{L}(\mathbf{u})\cdot(\mu^{-1}\nabla_h\times\mathbf{v})\,d\mathbf{x}\\ &\quad - \int_\Omega \mathcal{L}(\mathbf{v})\cdot(\mu^{-1}\nabla_h\times\mathbf{u})\,d\mathbf{x} + \int_{\mathcal{F}_h} \mathsf{a}\,[\![\mathbf{u}]\!]_T\cdot[\![\mathbf{v}]\!]_T\,ds,\\ \widetilde{b}_h(\mathbf{v},p) &= -\int_\Omega \varepsilon\mathbf{v}\cdot[\nabla_h p - \mathcal{M}(p)]\,d\mathbf{x}.\end{aligned}$$

Note that $a_h = \widetilde{a}_h$ in $\mathbf{V}_h\times\mathbf{V}_h$ and $b_h = \widetilde{b}_h$ in $\mathbf{V}_h\times Q_h$, although this is no longer true in $\mathbf{V}(h)\times\mathbf{V}(h)$ and in $\mathbf{V}(h)\times Q(h)$, respectively.

With this notation, we now consider the following auxiliary mixed formulation: find $(\mathbf{u}_h,p_h)$ in $\mathbf{V}_h\times Q_h$ such that

$$\widetilde{a}_h(\mathbf{u}_h,\mathbf{v}) + \widetilde{b}_h(\mathbf{v},p_h) = \textstyle\int_\Omega \mathbf{j}\cdot\mathbf{v}\,d\mathbf{x}, \tag{10a}$$

$$\widetilde{b}_h(\mathbf{u}_h,q) - c_h(p_h,q) = 0 \tag{10b}$$

for all $(\mathbf{v},q)\in\mathbf{V}_h\times Q_h$.

5.2. Continuity and stability properties

We begin by recalling the following continuity properties from [8, Section 5.1].

PROPOSITION 3. *The following results hold.*

(i) The forms $\widetilde{a}_h:\mathbf{V}(h)\times\mathbf{V}(h)\to\mathbb{R}$ *and* $\widetilde{b}_h:\mathbf{V}(h)\times Q(h)\to\mathbb{R}$ *are continuous with continuity constants independent of the mesh size and the coefficients* μ *and* ε.

(ii) The linear functional on the right-hand side of (10a) satisfies

$$\left|\int_\Omega \mathbf{j}\cdot\mathbf{v}\,d\mathbf{x}\right| \leq \varepsilon_*^{-\frac{1}{2}}\|\mathbf{j}\|_{0,\Omega}\|\mathbf{v}\|_{\mathbf{V}(h)},$$

for any $\mathbf{v}\in\mathbf{V}_h$.

Next, let us state some stability properties of the forms $\widetilde{a}_h$ and $\widetilde{b}_h$ on the conforming spaces $\mathbf{V}_h^c$ and Q_h^c in the decompositions defined in (7). To this end, we need to define the discrete kernel

$$\mathbf{Z}_h = \{\mathbf{v}\in\mathbf{V}_h : b_h(\mathbf{v},q) = 0\ \forall q\in Q_h^c\}. \tag{11}$$

LEMMA 1. *The following properties hold:*

(i) For parameters α *in (5) with* $\alpha>\alpha_0$, *there exists a positive constant* C, *independent of the mesh size, such that* $\widetilde{a}_h(\mathbf{v},\mathbf{v})\geq C\|\mathbf{v}\|^2_{\mathbf{V}(h)}$, *for any* $\mathbf{v}\in\mathbf{V}_h^c\cap\mathbf{Z}_h$.

(ii) The inf-sup condition

$$\inf_{q\in Q_h^c\setminus\{0\}} \sup_{\mathbf{v}\in\mathbf{V}_h^c} \frac{\widetilde{b}_h(\mathbf{v},q)}{\|\mathbf{v}\|_{\mathbf{V}(h)}\|q\|_{Q(h)}} \geq C > 0 \qquad (12)$$

holds, with a constant C independent of the mesh size and the coefficients μ and ε.

Proof. (i) The ellipticity property follows from Proposition 1 and the discrete Poincaré-Friedrich's inequality $\|\mathbf{v}\|_{0,\Omega} \leq C\,\|\nabla\times\mathbf{v}\|_{0,\Omega}$ for all $\mathbf{v}\in\mathbf{V}_h^c\cap\mathbf{Z}_h$, with a positive constant C independent of the mesh size and the coefficients μ and ε. This inequality can be proved using an analogous argument to the one presented in [6, Theorem 4.7], where the case of Nédéléc elements of the first type is considered; see also Monk [11, Corollary 4.8].

(ii) To prove the inf-sup condition in (12), we first fix $q\in Q_h^c$. Then, we choose $\mathbf{v}=-\nabla q$ and observe that $\mathbf{v}\in\mathbf{V}_h^c$. Thus,

$$\widetilde{b}_h(\mathbf{v},q) = \int_\Omega \varepsilon|\nabla q|^2\,d\mathbf{x} = \|q\|_{Q(h)}^2.$$

On the other hand, since $\nabla\times\mathbf{v}=0$ and $[\![\mathbf{v}]\!]_T=\mathbf{0}$,

$$\|\mathbf{v}\|_{\mathbf{V}(h)}^2 = \|\varepsilon^{\frac{1}{2}}\nabla q\|_{0,\Omega}^2 = \|q\|_{Q(h)}^2.$$

Thereby, (12) holds with an inf-sup constant $C=1$. □

REMARK 3. *Since $\mathbf{V}_h^c\subset\mathbf{V}_h$, the inf-sup condition (12) remains valid when $\mathbf{V}_h^c$ is replaced by $\mathbf{V}_h$, with the same inf-sup constant.*

6. Error estimates

In this section, we prove the error bound stated in Theorem 1. Our analysis closely follows the outline of the classical error analysis for conforming mixed methods (see, e.g., [3]), combined with ideas similar to those in [4] that allow us to use the stability properties of the forms in the conforming spaces $\mathbf{V}_h^c$ and Q_h^c underlying $\mathbf{V}_h$ and Q_h, respectively. To this end, we use the decomposition results of Theorem 2 throughout the proof.

6.1. Residuals

Recalling that $(\mathbf{u}, p)$ denotes the analytical solution of (1), we introduce the residuals

$$\begin{aligned} \mathcal{R}_1(\mathbf{u}, p; \mathbf{v}) &= \textstyle\int_\Omega \mathbf{j} \cdot \mathbf{v} \, d\mathbf{x} - \widetilde{a}_h(\mathbf{u}, \mathbf{v}) - \widetilde{b}_h(\mathbf{v}, p), \qquad (13)\\ \mathcal{R}_2(\mathbf{u}, p; q) &\equiv \mathcal{R}_2(\mathbf{u}; q) = \widetilde{b}_h(\mathbf{u}, q), \qquad (14) \end{aligned}$$

for any $(\mathbf{v}, q) \in \mathbf{V}_h \times Q_h$.

Writing $\mathbf{\Pi}_{\mathbf{V}_h}$ to denote the L^2–projection onto $\mathbf{V}_h$, we have the following bounds on the residuals.

PROPOSITION 4. *Assuming that the regularity assumptions stated in (6) hold; then, for any $\delta > 0$ there is a positive constant C_δ, independent of the mesh size, such that*

$$\begin{aligned} |\mathcal{R}_1(\mathbf{u}, p; \mathbf{v})| &\leq \delta^{-1} \|\mathbf{v}^\perp\|^2_{\mathbf{V}(h)} \\ &\quad + C_\delta \sum_{K \in \mathcal{T}_h} h_K \|\mu^{-1} \nabla \times \mathbf{u} - \mathbf{\Pi}_{\mathbf{V}_h}(\mu^{-1} \nabla \times \mathbf{u})\|^2_{0,\partial K}, \\ |\mathcal{R}_2(\mathbf{u}; q)| &\leq \delta^{-1} \|q^\perp\|^2_{Q(h)} + C_\delta \sum_{K \in \mathcal{T}_h} h_K \|\varepsilon \mathbf{u} - \mathbf{\Pi}_{\mathbf{V}_h}(\varepsilon \mathbf{u})\|^2_{0,\partial K}, \end{aligned}$$

for any $\mathbf{v} \in \mathbf{V}_h$ and $q \in Q_h$.

Proof. Assuming that the smoothness assumptions (6) hold, for $\mathbf{v} = \mathbf{v}^c \oplus \mathbf{v}^\perp \in \mathbf{V}_h$ and $q = q^c \oplus q^\perp \in Q_h$, we have that

$$\begin{aligned} |\mathcal{R}_1(\mathbf{u}, p; \mathbf{v})| &= \left| \int_{\mathcal{F}_h} \{\!\{\mu^{-1} \nabla \times \mathbf{u} - \mathbf{\Pi}_{\mathbf{V}_h}(\mu^{-1} \nabla \times \mathbf{u})\}\!\} \cdot [\![\mathbf{v}^\perp]\!]_T \, ds \right|, \\ |\mathcal{R}_2(\mathbf{u}; q)| &= \left| \int_{\mathcal{F}_h} \{\!\{\varepsilon \mathbf{u} - \mathbf{\Pi}_{\mathbf{V}_h}(\varepsilon \mathbf{u})\}\!\} \cdot [\![q^\perp]\!]_N \, ds \right|; \end{aligned}$$

see [8, Proposition 6.2] for details. Employing the Cauchy-Schwarz inequality, the bounds in (2), the shape-regularity of the mesh, and the norm-equivalence (8) in Theorem 2, we get

$$\begin{aligned} &|\mathcal{R}_1(\mathbf{u}, p; \mathbf{v})| \\ &\quad \leq C \left(\sum_{K \in \mathcal{T}_h} h_K \|\mu^{-1} \nabla \times \mathbf{u} - \mathbf{\Pi}_{\mathbf{V}_h}(\mu^{-1} \nabla \times \mathbf{u})\|^2_{0,\partial K} \right)^{\frac{1}{2}} \\ &\qquad \times \|\mathtt{m}^{-\frac{1}{2}} \mathtt{h}^{-\frac{1}{2}} [\![\mathbf{v}^\perp]\!]_T\|_{0,\mathcal{F}_h} \\ &\quad \leq C \left(\sum_{K \in \mathcal{T}_h} h_K \|\mu^{-1} \nabla \times \mathbf{u} - \mathbf{\Pi}_{\mathbf{V}_h}(\mu^{-1} \nabla \times \mathbf{u})\|^2_{0,\partial K} \right)^{\frac{1}{2}} \|\mathbf{v}^\perp\|_{\mathbf{V}(h)}. \end{aligned}$$

The arithmetic-geometric mean inequality completes the proof for $\mathcal{R}_1$; the bound for $\mathcal{R}_2$ is obtained analogously. □

6.2. A bound for $\|\mathbf{u}_h^\perp\|_{\mathbf{V}(h)}$ and $\|p_h^\perp\|_{Q(h)}$

We prove the following bound.

PROPOSITION 5. *Assume that the regularity assumptions stated in (6) hold. We let $(\mathbf{u}_h, p_h)$ be the solution of (4), with $\alpha > \alpha_0$ and $\gamma > 0$, and consider the decompositions $\mathbf{u}_h = \mathbf{u}_h^c + \mathbf{u}_h^\perp$ and $p_h = p_h^c + p_h^\perp$, according to (7). Then for any $\delta > 0$, there exists a positive constant C_δ, independent of the mesh size, such that*

$$\begin{aligned}\|\mathbf{u}_h^\perp\|^2_{\mathbf{V}(h)} + \|p_h^\perp\|^2_{Q(h)} \ &\leq \ \delta^{-1}\|\mathbf{u}-\mathbf{u}_h\|^2_{\mathbf{V}(h)} \\ &\qquad + C_\delta\left[\|\mathbf{u}-\mathbf{v}\|^2_{\mathbf{V}(h)} + \|p-q\|^2_{Q(h)} + \mathcal{E}(\mathbf{u})^2\right],\end{aligned}$$

for any $\mathbf{v} \in \mathbf{V}_h^c$ and any $q \in Q_h^c$. Here,

$$\begin{aligned}\mathcal{E}(\mathbf{u})^2 \ = \ \sum_{K\in\mathcal{T}_h} h_K &\Big[\|\mu^{-1}\nabla\times\mathbf{u} - \mathbf{\Pi}_{\mathbf{V}_h}(\mu^{-1}\nabla\times\mathbf{u})\|^2_{0,\partial K} \\ &+ \|\varepsilon\mathbf{u} - \mathbf{\Pi}_{\mathbf{V}_h}(\varepsilon\mathbf{u})\|^2_{0,\partial K}\Big]. \end{aligned} \tag{15}$$

Proof. We proceed in the following two steps.

Step 1. Let $\mathbf{w} \in \mathbf{V}_h^c \cap \mathbf{Z}_h$ and $q \in Q_h^c$, where $\mathbf{Z}_h$ is the kernel defined in (11). Using the norm-equivalence (8) of Theorem 2, the continuity of the tangential component of $\mathbf{u}_h^c$ and $\mathbf{w}$ at inter-element boundaries, and the ellipticity of the form $\widetilde{a}_h$ in the seminorm $|\cdot|_{\mathbf{V}(h)}$ for discrete functions (see Proposition 1), we deduce that

$$C_1\,\|\mathbf{u}_h^\perp\|^2_{\mathbf{V}(h)} \leq \|\mathbf{u}_h^\perp\|^2_{\mathbf{V}_h^\perp} \leq |\mathbf{u}_h - \mathbf{w}|^2_{\mathbf{V}(h)} \leq C\,\widetilde{a}_h(\mathbf{u}_h-\mathbf{w},\mathbf{u}_h-\mathbf{w}).$$

Thereby, using the norm equivalence (9), we get

$$\begin{aligned}\|\mathbf{u}_h^\perp\|^2_{\mathbf{V}(h)} + \|p_h^\perp\|^2_{Q(h)} \ &\leq \ C\,\left[\widetilde{a}_h(\mathbf{u}_h-\mathbf{w},\mathbf{u}_h-\mathbf{w}) + c_h(p_h^\perp,p_h^\perp)\right] \\ &\leq \ C\,\left[\widetilde{a}_h(\mathbf{u}_h-\mathbf{u},\mathbf{u}_h-\mathbf{w}) + \widetilde{a}_h(\mathbf{u}-\mathbf{w},\mathbf{u}_h-\mathbf{w})\right. \\ &\qquad \left. + c_h(p_h^\perp,p_h^\perp)\right].\end{aligned} \tag{16}$$

Let us first deal with the term $\widetilde{a}_h(\mathbf{u}_h-\mathbf{u},\mathbf{u}_h-\mathbf{w})$. To this end, from equation (10a) and the definition of the residual $\mathcal{R}_1$ in (13), we have

$$\begin{aligned}\widetilde{a}_h(\mathbf{u}_h-\mathbf{u},\mathbf{u}_h-\mathbf{w}) \ &= \ \mathcal{R}_1(\mathbf{u},p;\mathbf{u}_h-\mathbf{w}) + \widetilde{b}_h(\mathbf{u}_h-\mathbf{w},p-p_h) \\ &= \ \mathcal{R}_1(\mathbf{u},p;\mathbf{u}_h-\mathbf{w}) + \widetilde{b}_h(\mathbf{u}_h-\mathbf{w},p-p_h^c) \\ &\qquad - \widetilde{b}_h(\mathbf{u}_h-\mathbf{w},p_h^\perp).\end{aligned} \tag{17}$$

Since $\mathbf{u}_h-\mathbf{w}\in\mathbf{Z}_h$, we have that $\widetilde{b}_h(\mathbf{u}_h-\mathbf{w},p-p_h^c)=\widetilde{b}_h(\mathbf{u}_h-\mathbf{w},p-q)$, for any $q\in Q_h^c$. Employing equation (10b), the definition of the residual $\mathcal{R}_2$ in (14), and the fact that the jumps in p_h^c vanish, we obtain

$$\begin{aligned}-\widetilde{b}_h(\mathbf{u}_h-\mathbf{w},p_h^\perp) &= -\widetilde{b}_h(\mathbf{u}_h,p_h^\perp)-\widetilde{b}_h(\mathbf{u}-\mathbf{w},p_h^\perp)+\widetilde{b}_h(\mathbf{u},p_h^\perp)\\ &= -c_h(p_h^\perp,p_h^\perp)-\widetilde{b}_h(\mathbf{u}-\mathbf{w},p_h^\perp)+\mathcal{R}_2(\mathbf{u};p_h^\perp).\end{aligned}$$

Combining these identities with (16) gives

$$\begin{aligned}\|\mathbf{u}_h^\perp\|^2_{\mathbf{V}(h)}+\|p_h^\perp\|^2_{Q(h)}\le C\Big[&|\widetilde{a}_h(\mathbf{u}-\mathbf{w},\mathbf{u}_h-\mathbf{w})|+|\widetilde{b}_h(\mathbf{u}-\mathbf{w},p_h^\perp)|\\ &+|\widetilde{b}_h(\mathbf{u}_h-\mathbf{w},p-q)|+|\mathcal{R}_1(\mathbf{u},p;\mathbf{u}_h-\mathbf{w})|+|\mathcal{R}_2(\mathbf{u};p_h^\perp)|\Big].\end{aligned}$$

We can choose the parameter δ in the residual estimates derived in Proposition 4 in such a way that

$$\begin{aligned}\|\mathbf{u}_h^\perp\|^2_{\mathbf{V}(h)}+\|p_h^\perp\|^2_{Q(h)}\le C\Big[&|\widetilde{a}_h(\mathbf{u}-\mathbf{w},\mathbf{u}_h-\mathbf{w})|+|\widetilde{b}_h(\mathbf{u}-\mathbf{w},p_h^\perp)|\\ &+|\widetilde{b}_h(\mathbf{u}_h-\mathbf{w},p-q)|+\mathcal{E}(\mathbf{u})^2\Big]+\frac{1}{2}\Big[\|\mathbf{u}_h^\perp\|^2_{\mathbf{V}(h)}+\|p_h^\perp\|^2_{Q(h)}\Big].\end{aligned}$$

Therefore,

$$\begin{aligned}\|\mathbf{u}_h^\perp\|^2_{\mathbf{V}(h)}+\|p_h^\perp\|^2_{Q(h)} \le\ & C\Big[|\widetilde{a}_h(\mathbf{u}-\mathbf{w},\mathbf{u}_h-\mathbf{w})|+|\widetilde{b}_h(\mathbf{u}-\mathbf{w},p_h^\perp)|\\ &+|\widetilde{b}_h(\mathbf{u}_h-\mathbf{w},p-q)|+\mathcal{E}(\mathbf{u})^2\Big].\end{aligned}$$

Employing the continuity of the forms $\widetilde{a}_h$ and $\widetilde{b}_h$ stated in Proposition 3, the triangle inequality $\|\mathbf{u}_h-\mathbf{w}\|_{\mathbf{V}(h)}\le\|\mathbf{u}-\mathbf{u}_h\|_{\mathbf{V}(h)}+\|\mathbf{u}-\mathbf{w}\|_{\mathbf{V}(h)}$, and the arithmetic-geometric mean inequality, we deduce that, for $\delta>0$,

$$\begin{aligned}&\|\mathbf{u}_h^\perp\|^2_{\mathbf{V}(h)}+\|p_h^\perp\|^2_{Q(h)}\\ &\quad\le C\Big[\|\mathbf{u}-\mathbf{w}\|_{\mathbf{V}(h)}\|\mathbf{u}_h-\mathbf{w}\|_{\mathbf{V}(h)}+\|\mathbf{u}-\mathbf{w}\|_{\mathbf{V}(h)}\|p_h^\perp\|_{Q(h)}\\ &\qquad+\|\mathbf{u}_h-\mathbf{w}\|_{\mathbf{V}(h)}\|p-q\|_{Q(h)}+\mathcal{E}(\mathbf{u})^2\Big]\\ &\quad\le C\Big[\|\mathbf{u}-\mathbf{w}\|_{\mathbf{V}(h)}\|\mathbf{u}-\mathbf{u}_h\|_{\mathbf{V}(h)}+\|\mathbf{u}-\mathbf{w}\|^2_{\mathbf{V}(h)}\\ &\qquad+\|\mathbf{u}-\mathbf{w}\|_{\mathbf{V}(h)}\|p_h^\perp\|_{Q(h)}+\|\mathbf{u}-\mathbf{u}_h\|_{\mathbf{V}(h)}\|p-q\|_{Q(h)}\\ &\qquad+\|\mathbf{u}-\mathbf{w}\|_{\mathbf{V}(h)}\|p-q\|_{Q(h)}+\mathcal{E}(\mathbf{u})^2\Big]\\ &\quad\le\frac{1}{2\delta}\|\mathbf{u}-\mathbf{u}_h\|^2_{\mathbf{V}(h)}+C_\delta\|\mathbf{u}-\mathbf{w}\|^2_{\mathbf{V}(h)}+C_\delta\|p-q\|^2_{Q(h)}\\ &\qquad+\frac{1}{2}\|p_h^\perp\|^2_{Q(h)}+C\,\mathcal{E}(\mathbf{u})^2.\end{aligned}$$

Subtracting $\frac{1}{2}\|p_h^\perp\|_{Q(h)}^2$ from both sides and multiplying by a factor 2, we conclude that

$$\begin{aligned}
&\|\mathbf{u}_h^\perp\|_{\mathbf{V}(h)}^2 + \|p_h^\perp\|_{Q(h)}^2 \\
&\quad \le \delta^{-1}\|\mathbf{u} - \mathbf{u}_h\|_{\mathbf{V}(h)}^2 + C_\delta \left[\|\mathbf{u} - \mathbf{w}\|_{\mathbf{V}(h)}^2 + \|p - q\|_{Q(h)}^2 + \mathcal{E}(\mathbf{u})^2\right], \quad (18)
\end{aligned}$$

for any $\mathbf{w} \in \mathbf{V}_h^c \cap \mathbf{Z}_h$, and any $q \in Q_h^c$.

Step 2. We now show that $\mathbf{w} \in \mathbf{V}_h^c \cap \mathbf{Z}_h$ can be replaced by any $\mathbf{v} \in \mathbf{V}_h^c$ in (18). To this end, we let $\mathbf{v} \in \mathbf{V}_h^c$ and choose $\mathbf{r} \in \mathbf{V}_h^c$ such that

$$\begin{aligned}
&\widetilde{b}_h(\mathbf{r}, s) = \widetilde{b}_h(\mathbf{u} - \mathbf{v}, s) \qquad \forall s \in Q_h^c, \\
&\|\mathbf{r}\|_{\mathbf{V}(h)} \le C\,\|\mathbf{u} - \mathbf{v}\|_{\mathbf{V}(h)}.
\end{aligned}$$

The inf-sup condition for $\mathbf{V}_h^c \times Q_h^c$ in Lemma 1 guarantees that this problem admits at least one solution $\mathbf{r} \in \mathbf{V}_h^c$. Then, we can set $\mathbf{w} = \mathbf{r} + \mathbf{v}$; note, by construction, that $\mathbf{w} \in \mathbf{V}_h^c \cap \mathbf{Z}_h$, since $\widetilde{b}_h(\mathbf{u}, s) = 0$ for any $s \in Q_h^c$. Inserting $\mathbf{w}$ in (18) gives

$$\begin{aligned}
&\|\mathbf{u}_h^\perp\|_{\mathbf{V}(h)}^2 + \|p_h^\perp\|_{Q(h)}^2 \\
&\quad \le \delta^{-1}\|\mathbf{u} - \mathbf{u}_h\|_{\mathbf{V}(h)}^2 + C_\delta \left[\|\mathbf{u} - \mathbf{v}\|_{\mathbf{V}(h)}^2 + \|\mathbf{r}\|_{\mathbf{V}(h)}^2 \right. \\
&\qquad\qquad \left. + \|p - q\|_{Q(h)}^2 + \mathcal{E}(\mathbf{u})^2\right] \\
&\quad \le \delta^{-1}\|\mathbf{u} - \mathbf{u}_h\|_{\mathbf{V}(h)}^2 + C_\delta \left[\|\mathbf{u} - \mathbf{v}\|_{\mathbf{V}(h)}^2 + \|p - q\|_{Q(h)}^2 + \mathcal{E}(\mathbf{u})^2\right],
\end{aligned}$$

which completes the proof. □

6.3. Error in u

We are now ready to prove the following bound for the error in the approximation to the vector-valued variable $\mathbf{u}$.

PROPOSITION 6. *Suppose that the analytical solution $(\mathbf{u}, p)$ of (1) satisfies (6). Then, the DG approximation $(\mathbf{u}_h, p_h)$ defined in (4), with $\alpha > \alpha_0$ and $\gamma > 0$, satisfies the error bound*

$$\|\mathbf{u} - \mathbf{u}_h\|_{\mathbf{V}(h)}^2 \le C\,\left[\|\mathbf{u} - \mathbf{v}\|_{\mathbf{V}(h)}^2 + \|p - q\|_{Q(h)}^2 + \mathcal{E}(\mathbf{u})^2\right],$$

for any $\mathbf{v} \in \mathbf{V}_h^c$ and $q \in Q_h^c$, where C is a positive constant, independent of the the mesh size h, and $\mathcal{E}(\mathbf{u})$ is the expression defined in (15).

Proof. We proceed in the following two steps.

Step 1: We decompose the discrete solution $\mathbf{u}_h$ as $\mathbf{u}_h = \mathbf{u}_h^c + \mathbf{u}_h^\perp$, according to (7); then, using the triangle inequality, we have

$$\|\mathbf{u} - \mathbf{u}_h\|_{\mathbf{V}(h)}^2 \leq C \left[\|\mathbf{u} - \mathbf{u}_h^c\|_{\mathbf{V}(h)}^2 + \|\mathbf{u}_h^\perp\|_{\mathbf{V}(h)}^2 \right]. \tag{19}$$

We start by estimating the first term on the right-hand side of (19).

Since $\widetilde{b}_h(\mathbf{u}_h, s) = 0$, for any $s \in Q_h^c$, we have that $\widetilde{b}_h(\mathbf{u}_h^c, s) = -\widetilde{b}_h(\mathbf{u}_h^\perp, s)$, for any $s \in Q_h^c$. Let $\mathbf{w} \in \mathbf{V}_h^c$ be such that

$$\widetilde{b}_h(\mathbf{w}, s) = -\widetilde{b}_h(\mathbf{u}_h^\perp, s) \qquad \forall s \in Q_h^c. \tag{20}$$

The inf-sup condition for $\mathbf{V}_h^c \times Q_h^c$ in Lemma 1 guarantees that problem (20) admits at least one solution $\mathbf{w} \in \mathbf{V}_h^c$. It follows that $\mathbf{u}_h^c - \mathbf{w}$ belongs to $\mathbf{V}_h^c \cap \mathbf{Z}_h$. Then, owing to the coercivity property in Lemma 1 and the identity $\mathbf{u}_h = \mathbf{u}_h^c + \mathbf{u}_h^\perp$, we have

$$\begin{aligned} C\,\|\mathbf{u}_h^c - \mathbf{w}\|_{\mathbf{V}(h)}^2 &\leq \widetilde{a}_h(\mathbf{u}_h^c - \mathbf{w}, \mathbf{u}_h^c - \mathbf{w}) \\ &= \widetilde{a}_h(\mathbf{u}_h^c - \mathbf{w}, \mathbf{u} - \mathbf{w}) + \widetilde{a}_h(\mathbf{u}_h^c - \mathbf{w}, \mathbf{u}_h - \mathbf{u}) \\ &\quad -\widetilde{a}_h(\mathbf{u}_h^c - \mathbf{w}, \mathbf{u}_h^\perp). \end{aligned}$$

Using equation (10a) and the definition of the residual $\mathcal{R}_1$ in (13), we obtain

$$\begin{aligned} \widetilde{a}_h(\mathbf{u}_h^c - \mathbf{w}, \mathbf{u}_h - \mathbf{u}) &= \mathcal{R}_1(\mathbf{u}, p; \mathbf{u}_h^c - \mathbf{w}) + \widetilde{b}_h(\mathbf{u}_h^c - \mathbf{w}, p - p_h^c) \\ &\quad -\widetilde{b}_h(\mathbf{u}_h^c - \mathbf{w}, p_h^\perp), \end{aligned}$$

cf. (17) above. Since $\mathbf{u}_h^c - \mathbf{w}$ is in $H_0(\mathrm{curl};\Omega)$, we have $\mathcal{R}_1(\mathbf{u}, p; \mathbf{u}_h^c - \mathbf{w}) = 0$; see the proof of Proposition 4. Recalling that $\mathbf{u}_h^c - \mathbf{w} \in \mathbf{V}_h^c \cap \mathbf{Z}_h$, we have

$$\widetilde{a}_h(\mathbf{u}_h^c - \mathbf{w}, \mathbf{u}_h - \mathbf{u}) = \widetilde{b}_h(\mathbf{u}_h^c - \mathbf{w}, p - q) - \widetilde{b}_h(\mathbf{u}_h^c - \mathbf{w}, p_h^\perp),$$

for any $q \in Q_h^c$. Consequently, using the results stated in Proposition 3, we get

$$\|\mathbf{u}_h^c - \mathbf{w}\|_{\mathbf{V}(h)} \leq C \left[\|\mathbf{u} - \mathbf{w}\|_{\mathbf{V}(h)} + \|p - q\|_{Q(h)} + \|\mathbf{u}_h^\perp\|_{\mathbf{V}(h)} + \|p_h^\perp\|_{Q(h)} \right],$$

for any $q \in Q_h^c$. Employing the triangle inequality

$$\|\mathbf{u} - \mathbf{u}_h^c\|_{\mathbf{V}(h)} \leq \|\mathbf{u} - \mathbf{w}\|_{\mathbf{V}(h)} + \|\mathbf{u}_h^c - \mathbf{w}\|_{\mathbf{V}(h)},$$

together with the above inequality gives

$$\|\mathbf{u} - \mathbf{u}_h^c\|_{\mathbf{V}(h)}^2 \leq C \left[\|\mathbf{u} - \mathbf{w}\|_{\mathbf{V}(h)}^2 + \|p - q\|_{Q(h)}^2 + \|\mathbf{u}_h^\perp\|_{\mathbf{V}(h)}^2 + \|p_h^\perp\|_{Q(h)}^2 \right].$$

Then, inserting this result into (19), we obtain

$$\|\mathbf{u}-\mathbf{u}_h\|^2_{\mathbf{V}(h)} \le C\Big[\|\mathbf{u}-\mathbf{w}\|^2_{\mathbf{V}(h)} + \|p-q\|^2_{Q(h)} + \|\mathbf{u}_h^\perp\|^2_{\mathbf{V}(h)} + \|p_h^\perp\|^2_{Q(h)}\Big], \tag{21}$$

for any $\mathbf{w} \in \mathbf{V}_h^c$ that satisfies (20), and any $q \in Q_h^c$.

Step 2: Now, let $\mathbf{v} \in V_h^c$ be arbitrary and $\mathbf{r} \in \mathbf{V}_h^c$ be such that

$$\begin{aligned}
&\widetilde{b}_h(\mathbf{r}, s) = \widetilde{b}_h(\mathbf{u}-\mathbf{v}-\mathbf{u}_h^\perp, s) \qquad \forall s \in Q_h^c,\\
&\|\mathbf{r}\|^2_{\mathbf{V}(h)} \le C\,\Big(\|\mathbf{u}-\mathbf{v}\|^2_{\mathbf{V}(h)} + \|\mathbf{u}_h^\perp\|^2_{\mathbf{V}(h)}\Big).
\end{aligned}$$

The inf-sup condition for $\mathbf{V}_h^c \times Q_h^c$ in Lemma 1 guarantees that this problem admits at least one solution $\mathbf{r} \in \mathbf{V}_h^c$. Defining $\mathbf{w} = \mathbf{r}+\mathbf{v}$, we have that $\mathbf{w} \in \mathbf{V}_h^c$; moreover $\mathbf{w}$ satisfies (20). Since $\widetilde{b}_h(\mathbf{w}, s) = \widetilde{b}_h(\mathbf{r}+\mathbf{v}, s) = \widetilde{b}_h(\mathbf{u}-\mathbf{u}_h^\perp, s) = -\widetilde{b}_h(\mathbf{u}_h^\perp, s)$, because $\widetilde{b}_h(\mathbf{u}, s) = 0$ for any $s \in Q_h^c$. Therefore, $\mathbf{w} = \mathbf{r}+\mathbf{v}$ can be inserted in (21) and we get

$$\begin{aligned}
&\|\mathbf{u}-\mathbf{u}_h\|^2_{\mathbf{V}(h)}\\
&\quad\le C\Big[\|\mathbf{u}-\mathbf{v}\|^2_{\mathbf{V}(h)} + \|\mathbf{r}\|^2_{\mathbf{V}(h)} + \|p-q\|^2_{Q(h)} + \|\mathbf{u}_h^\perp\|^2_{\mathbf{V}_h^\perp} + \|p_h^\perp\|^2_{Q(h)}\Big]\\
&\quad\le C\Big[\|\mathbf{u}-\mathbf{v}\|^2_{\mathbf{V}(h)} + \|p-q\|^2_{Q(h)} + \|\mathbf{u}_h^\perp\|^2_{\mathbf{V}(h)} + \|p_h^\perp\|^2_{Q(h)}\Big],
\end{aligned}$$

for any $q \in Q_h^c$. Employing the result of Proposition 5, with $\delta = 2C$, we obtain

$$\|\mathbf{u}-\mathbf{u}_h\|^2_{\mathbf{V}(h)} \le C\left[\|\mathbf{u}-\mathbf{v}\|^2_{\mathbf{V}(h)} + \|p-q\|^2_{Q(h)} + \mathcal{E}(\mathbf{u})^2\right] + \frac{1}{2}\|\mathbf{u}-\mathbf{u}_h\|^2_{\mathbf{V}(h)}.$$

Subtracting $\frac{1}{2}\|\mathbf{u}-\mathbf{u}_h\|^2_{\mathbf{V}(h)}$ from both sides of the above equation completes the proof of Proposition 6. □

6.4. Error in p

The proof of the error bound for the approximation to p is now a straightforward extension of the analogous one for conforming mixed methods.

PROPOSITION 7. *Suppose that the analytical solution $(\mathbf{u}, p)$ of (1) satisfies (6). Then, the DG approximation $(\mathbf{u}_h, p_h)$ defined in (4), with $\alpha > \alpha_0$ and $\gamma > 0$, satisfies the error bound*

$$\|p-p_h\|^2_{Q(h)} \le C\left[\|\mathbf{u}-\mathbf{v}\|^2_{\mathbf{V}(h)} + \|p-q\|^2_{Q(h)} + \mathcal{E}(\mathbf{u})^2\right],$$

for any $\mathbf{v} \in \mathbf{V}_h^c$ and $q \in Q_h^c$, where C is a positive constant, independent of the the mesh size h, and $\mathcal{E}(\mathbf{u})$ is the expression defined in (15).

Proof. Letting $q \in Q_h^c$, we note that

$$\|p - p_h\|_{Q(h)}^2 \le C \left[\|p - q\|_{Q(h)}^2 + \|q - p_h^c\|_{Q(h)}^2 + \|p_h^\perp\|_{Q(h)}^2 \right]. \qquad (22)$$

First, we estimate $\|q - p_h^c\|_{Q(h)}$; from the inf-sup condition in Lemma 1, we have

$$\begin{aligned} C\|q - p_h^c\|_{Q(h)} &\le \sup_{\mathbf{v} \in \mathbf{V}_h^c} \frac{\widetilde{b}_h(\mathbf{v}, q - p_h^c)}{\|\mathbf{v}\|_{\mathbf{V}(h)}} \\ &= \sup_{\mathbf{v} \in \mathbf{V}_h^c} \frac{\widetilde{b}_h(\mathbf{v}, q - p) + \widetilde{b}_h(\mathbf{v}, p - p_h) + \widetilde{b}(\mathbf{v}, p_h^\perp)}{\|\mathbf{v}\|_{\mathbf{V}(h)}}. \end{aligned}$$

From equation (10a), we have $\widetilde{b}_h(\mathbf{v}, p - p_h) = -\mathcal{R}_1(\mathbf{u}, p; \mathbf{v}) - \widetilde{a}_h(\mathbf{u} - \mathbf{u}_h, \mathbf{v})$, with the residual $\mathcal{R}_1$ defined in (13); thereby, $\widetilde{b}_h(\mathbf{v}, p - p_h) = -\widetilde{a}_h(\mathbf{u} - \mathbf{u}_h, \mathbf{v})$, since $\mathcal{R}_1(\mathbf{u}, p; \mathbf{v}) = 0$ for all $\mathbf{v} \in \mathbf{V}_h^c$. Exploiting the continuity of the forms $\widetilde{a}_h$ and $\widetilde{b}_h$, cf. Proposition 3, we obtain

$$\|q - p_h^c\|_{Q(h)}^2 \le C \left[\|\mathbf{u} - \mathbf{u}_h\|_{\mathbf{V}(h)}^2 + \|p - q\|_{Q(h)}^2 + \|p_h^\perp\|_{Q(h)}^2 \right].$$

Substituting the above expression into inequality (22) and using Proposition 5 yields

$$\|p - p_h\|_{Q(h)}^2 \le C \left[\|\mathbf{u} - \mathbf{u}_h\|_{\mathbf{V}(h)}^2 + \|\mathbf{u} - \mathbf{v}\|_{\mathbf{V}(h)}^2 + \|p - q\|_{Q(h)}^2 + \mathcal{E}(\mathbf{u})^2 \right].$$

Employing Proposition 6 completes the proof. □

6.5. Proof of Theorem 1

To complete the proof of Theorem 1, we first note that standard approximation properties for $\mathbf{V}_h^c$ and Q_h^c show that

$$\begin{aligned} &\inf_{\mathbf{v} \in \mathbf{V}_h^c} \|\mathbf{u} - \mathbf{v}\|_{\mathbf{V}(h)} + \inf_{q \in Q_h^c} \|p - q\|_{\mathbf{V}(h)} \\ &\qquad \le C\, h^{\min\{s,\ell\}} \left[\|\varepsilon \mathbf{u}\|_{s,\Omega} + \|\mu^{-1} \nabla \times \mathbf{u}\|_{s,\Omega} + \|p\|_{s+1,\Omega} \right]; \end{aligned}$$

see, e.g., [11] for details. Here, we also used the bounds in (2) on the coefficients ε and μ. Finally, the approximation properties for the L^2–projection yield

$$\mathcal{E}(\mathbf{u}) \le C\, h^{\min\{s,\ell\}} \left[\|\varepsilon \mathbf{u}\|_{s,\Omega} + \|\mu^{-1} \nabla \times \mathbf{u}\|_{s,\Omega} \right].$$

Substituting these inequalities into the error bounds derived in Propositions 6 and 7 completes the proof of Theorem 1.

7. Numerical results

In this section we present a series of numerical experiments to highlight the practical performance of the mixed DG method introduced in this article for the numerical approximation of the model problem (1). For simplicity, we restrict ourselves to two-dimensional model problems with constant coefficients $\mu \equiv \varepsilon \equiv 1$. Additionally, we note that throughout this section we select the constants appearing in the stabilization parameters defined in (5) as follows:

$$\alpha = 10\,\ell^2 \quad \text{and} \quad \gamma = 1.$$

We remark that the dependence of α on the polynomial degree ℓ has been formally chosen in order to guarantee the ellipticity property of the form a_h in Proposition 1 independently of ℓ, cf. [9], for example.

7.1. Example 1

In this first example we select $\Omega \subset \mathbb{R}^2$ to be the L–shaped domain with vertices $(1,0)$, $(1,1)$, $(-1,1)$, $(-1,-1)$, $(0,-1)$ and $(0,0)$. Furthermore, we choose $\mathbf{j}$ (and suitable non-homogeneous boundary conditions for $\mathbf{u}$) so that the analytical solution to the two-dimensional analogue of (1) with $\mu \equiv \varepsilon \equiv 1$ is given by

$$\begin{pmatrix} u_1 \\ u_2 \\ p \end{pmatrix} = \begin{pmatrix} -\exp(x)(y\cos(y)+\sin(y)) \\ \exp(x)y\sin(y) \\ \sin(\pi(x-1)/2)\sin(\pi(y-1)/2) \end{pmatrix};$$

cf. [8]. Here, we investigate the asymptotic convergence of the mixed DG method (4) on a sequence of successively finer uniform and quasi-uniform unstructured triangular meshes for $\ell = 1,2,3,4$. In each case the uniform meshes are constructed from a uniform square mesh by connecting the north east vertex with the south west one within each mesh square.

In Figures 1 and 2 we plot the norms $\|\cdot\|_{\mathbf{V}(h)}$ and $\|\cdot\|_{Q(h)}$ of the errors $\mathbf{u}-\mathbf{u}_h$ and $p-p_h$, respectively, with respect to the square root of the number of degrees of freedom in the finite element space $\mathbf{V}_h \times Q_h$. Here, we observe that $\|\mathbf{u}-\mathbf{u}_h\|_{\mathbf{V}(h)}$ converges to zero, for each fixed ℓ, at the optimal rate $\mathcal{O}(h^\ell)$, as the mesh is refined, in accordance with Theorem 1. On the other hand, for this mixed-order method, $\|p-p_h\|_{Q(h)}$ converges at the rate $\mathcal{O}(h^{\ell+1})$, for each ℓ, as h tends to zero; this rate is indeed optimal, though this is not reflected by Theorem 1. Additionally, from Figures 1 and 2 we observe that the accuracy of the proposed DG method is comparable on each of the two types of meshes employed here.

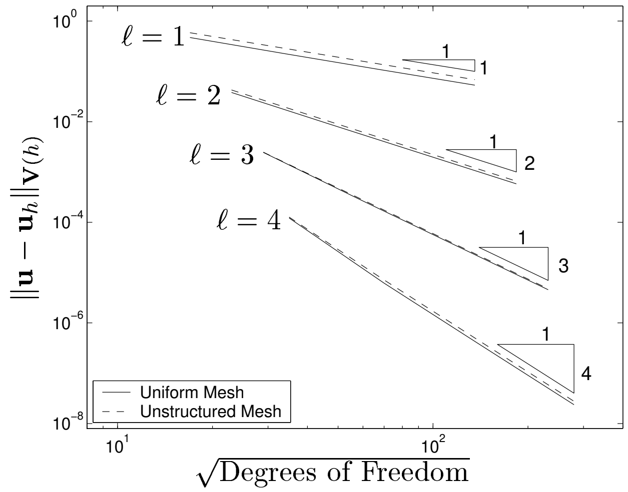

Figure 1. Example 1. Convergence of $\|\mathbf{u} - \mathbf{u}_h\|_{\mathbf{V}(h)}$.

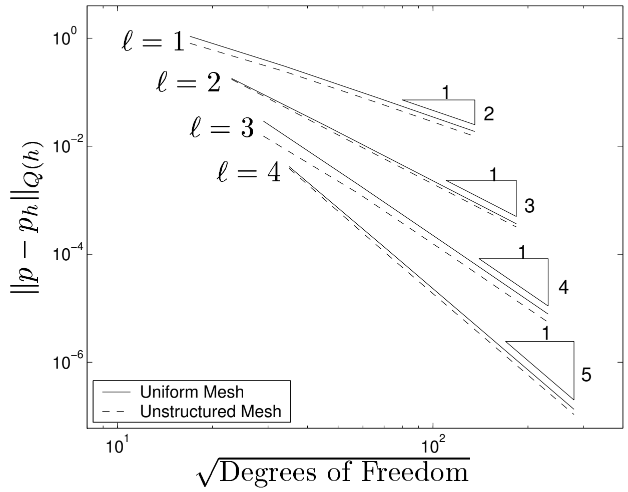

Figure 2. Example 1. Convergence of $\|p - p_h\|_{Q(h)}$.

Secondly, we highlight the optimality of the proposed mixed method when the error in the computed vector field $\mathbf{u}_h$ is measured in terms of the $L^2(\Omega)$-norm. We recall that the equal–order mixed DG method introduced and analyzed in [8] is suboptimal in this case by a full order of h; indeed, it was demonstrated numerically in [8] that when conforming meshes are employed, the $L^2(\Omega)$-norm of the error behaves like $\mathcal{O}(h^\ell)$, for each ℓ, as h tends to zero. On the other hand, Figure 3 demonstrates that the mixed-order method introduced in this

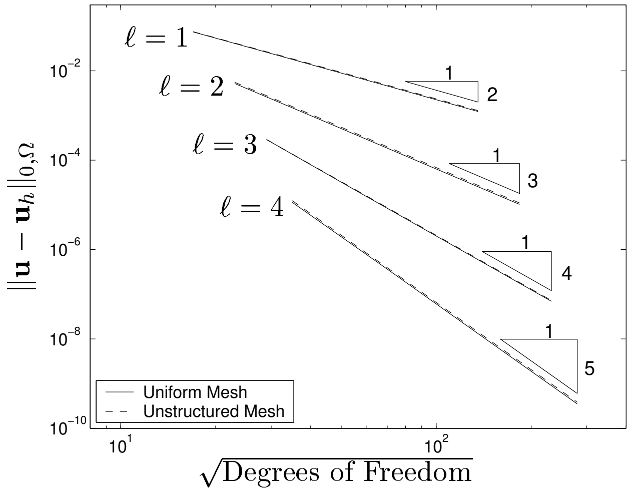

Figure 3. Example 1. Convergence of $\|\mathbf{u} - \mathbf{u}_h\|_{0,\Omega}$.

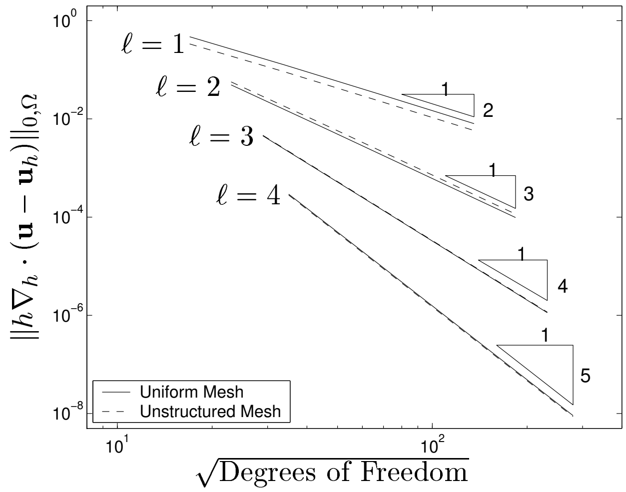

Figure 4. Example 1. Convergence of $\|h\nabla_h \cdot (\mathbf{u} - \mathbf{u}_h)\|_{0,\Omega}$.

article yields an optimal convergence rate for the above quantity as the mesh is refined. Analogous behavior is also observed when the $L^2(\Omega)$–norm of the error in the approximation to the (elementwise) divergence of $\mathbf{u}$ is computed. Indeed, from Figure 4, we observe that $\|h\,\nabla_h \cdot (\mathbf{u} - \mathbf{u}_h)\|_{0,\Omega} = (\sum_{K \in \mathcal{T}_h} h_K^2 \|\nabla \cdot (\mathbf{u} - \mathbf{u}_h)\|_{0,K}^2)^{1/2}$ converges to zero at the optimal rate $\mathcal{O}(h^{\ell+1})$ as h tends to zero, when both uniform and quasi-uniform triangular meshes are employed. We should point out that the DG method proposed in this article leads to an increase in

Table I. Example 2. Convergence of $\|\|(\mathbf{e_u}, e_p)\|\|_{\rm DG}$ on uniform triangular meshes with $n = 1$.

	$\ell = 1$		$\ell = 2$		$\ell = 3$	
Elements	$\|\|(\mathbf{e_u}, e_p)\|\|_{\rm DG}$	k	$\|\|(\mathbf{e_u}, e_p)\|\|_{\rm DG}$	k	$\|\|(\mathbf{e_u}, e_p)\|\|_{\rm DG}$	k
24	2.677	-	3.704	-	4.348	-
96	2.439	0.13	2.907	0.35	3.254	0.42
384	1.799	0.44	2.002	0.54	2.196	0.57
1536	1.196	0.59	1.300	0.62	1.417	0.63
6144	0.765	0.65	0.826	0.65	0.8989	0.66

the number of degrees of freedom employed for the numerical approximation of the variable p in comparison to the equal–order stabilized method introduced in [8]. However, this increase in complexity is relatively small, since p is only a scalar variable; moreover, given that resulting mixed–order method yields optimal convergence rates for the approximation to the *vector* variable $\mathbf{u}$, when the error is measured in the $L^2(\Omega)$-norm, this increase seems more than justified.

Finally, we remark that analogous results also hold on quadrilateral meshes when the discontinuous version of the first family of Nédélec's elements, cf. [12], are employed. For brevity, these numerics have been omitted; we refer, instead, to the recent article [7], where computational comparisons between triangular and square meshes have been performed.

7.2. Example 2

In this second example, we investigate the performance of the mixed DG method (4) for a problem in which the precise regularity of the analytical solution $\mathbf{u}$ is known. To this end, we again let Ω be the L-shaped domain employed in Example 1 above; here, we set $\mathbf{j} = \mathbf{0}$ and select the boundary condition $\mathbf{g}$ so that the analytical solution $\mathbf{u}$ to the two-dimensional analogue of (1) with $\mu \equiv \varepsilon \equiv 1$ is given, in terms of the polar coordinates (r, ϑ), by

$$\mathbf{u}(x,y) = \nabla S(r,\vartheta), \quad \text{where} \quad S(r,\vartheta) = r^{2n/3}\sin(2n\vartheta/3), \tag{23}$$

and $n \geq 1$ is a parameter; in this case $p \equiv 0$. The analytical solution given by (23) contains a singularity at the re-entrant corner located at the origin of Ω; here, we have $\mathbf{u} \in H^{2n/3-\varepsilon}(\Omega)^2$, $\varepsilon > 0$.

Table II. Example 2. Convergence of $\|\!|(\mathbf{e_u}, e_p)\|\!|_{\mathrm{DG}}$ on uniform triangular meshes with $n = 2$.

	$\ell = 1$		$\ell = 2$		$\ell = 3$	
Elements	$\|\!|(\mathbf{e_u}, e_p)\|\!|_{\mathrm{DG}}$	k	$\|\!|(\mathbf{e_u}, e_p)\|\!|_{\mathrm{DG}}$	k	$\|\!|(\mathbf{e_u}, e_p)\|\!|_{\mathrm{DG}}$	k
24	5.751e-1	-	3.730e-1	-	2.841e-1	-
96	2.583e-1	1.15	1.534e-1	1.28	1.149e-1	1.31
384	1.062e-1	1.28	6.146e-2	1.32	4.583e-2	1.33
1536	4.257e-2	1.32	2.445e-2	1.33	1.821e-2	1.33
6144	1.694e-2	1.33	9.708e-3	1.33	7.228e-3	1.33

Table III. Example 2. Convergence of $\|\!|(\mathbf{e_u}, e_p)\|\!|_{\mathrm{DG}}$ on uniform triangular meshes with $n = 3$.

	$\ell = 1$		$\ell = 2$		$\ell = 3$	
Elements	$\|\!|(\mathbf{e_u}, e_p)\|\!|_{\mathrm{DG}}$	k	$\|\!|(\mathbf{e_u}, e_p)\|\!|_{\mathrm{DG}}$	k	$\|\!|(\mathbf{e_u}, e_p)\|\!|_{\mathrm{DG}}$	k
24	1.532	-	8.253e-2	-	2.296e-2	-
96	4.119e-1	1.90	1.360e-2	2.60	3.700e-3	2.63
384	1.012e-1	2.03	2.183e-3	2.64	5.862e-4	2.66
1536	2.486e-2	2.03	3.470e-4	2.65	9.246e-5	2.66
6144	6.262e-3	1.99	5.494e-5	2.66	1.457e-5	2.67

In this example, we confine ourselves to uniform (structured) triangular meshes; analogous results also hold on unstructured meshes consisting of triangles, but for the sake of brevity, these results have been omitted. Before we proceed, let us first introduce some notation: we write $\mathbf{e_u}$ to denote the error $\mathbf{u} - \mathbf{u}_h$ in the vector variable and e_p to denote the error $p - p_h$ in the scalar field. In Tables I, II and III we present a comparison of the DG-norm of the error in the approximation to both $\mathbf{u}$ and p for $n = 1, 2, 3$, respectively, with the mesh function h on a sequence of uniform triangular meshes for $1 \leq \ell \leq 3$. In each case we show the number of elements in the computational mesh, the corresponding DG-norm of the error and the computed rate of convergence k. Here, we observe that (asymptotically) $\|\!|(\mathbf{e_u}, e_p)\|\!|_{\mathrm{DG}}$ converges to zero at the optimal rate $\mathcal{O}(h^{\min(2n/3-\varepsilon,\ell)})$, for each fixed n, as h tends to zero, as predicted by Theorem 1. One exception to this is when $n = 2$ and $\ell = 1$, cf. Table II, where the error actually tends to zero at the superior rate of $\mathcal{O}(h^{4/3})$ as h tends to zero.

8. Conclusions

In this paper we have studied a new mixed discontinuous Galerkin finite element method for the discretization of the time-harmonic Maxwell operator on simplicial meshes. In contrast to the stabilized method introduced and analyzed in [8], the proposed scheme is based on employing mixed–order finite element spaces for the approximation of the unknowns; this choice of spaces eliminates the need to penalize the normal jumps in the approximation to the vector unknown $\mathbf{u}$. Our error analysis and numerical results show that the proposed method is optimally convergent in the energy norm for both smooth as well as singular solutions. Moreover, in contrast to the equal–order method proposed in [8], numerical experiments presented in this article have indicated that this new mixed–order scheme is also optimally convergent when the error is measured in terms of the $L^2(\Omega)$-norm.

Appendix

To prove the norm-equivalence (8) in Theorem 2, we proceed in several steps. The key ingredient is the approximation result in Step 5; for scalar diffusion problems an analogous approximation result has been shown in [10, Theorem 2.2].

Step 1 (Preliminaries). We begin by introducing some definitions. Recall that each element $K \in \mathcal{T}_h$ is the image of the reference element $\widehat{K}$ under an affine mapping F_K; that is, $K = F_K(\widehat{K})$ for all $K \in \mathcal{T}_h$, where $F_K(\widehat{\mathbf{x}}) = B_K\widehat{\mathbf{x}} + \mathbf{b}_K$ and $B_K \in \mathbb{R}^{3\times 3}$, $\mathbf{b}_K \in \mathbb{R}^3$. Without loss of generality, we assume that $\det B_K > 0$. We define

$$\mathbb{D}^\ell(K) = \{\, \mathbf{q} \,:\, \mathbf{q}\circ F_K = \frac{1}{\det B_K} B_K\widehat{\mathbf{q}},\ \widehat{\mathbf{q}} \in \mathbb{P}^{\ell-1}(\widehat{K})^3 \oplus \widetilde{\mathbb{P}}^{\ell-1}(\widehat{K})\,\widehat{\mathbf{x}}\,\},$$

where $\widetilde{\mathbb{P}}^{\ell-1}(\widehat{K})$ denotes the space of homogeneous polynomials of total degree exactly $\ell - 1$ in $\widehat{\mathbf{x}} = (\widehat{x}_1, \widehat{x}_2, \widehat{x}_3)$ on $\widehat{K}$. A polynomial $\mathbf{q} \in \mathbb{D}^\ell(K)$ can be represented as $\mathbf{q}(\mathbf{x}) = \mathbf{r}(\mathbf{x}) + \widetilde{s}(\mathbf{x})\,\mathbf{x}$, with $\mathbf{r} \in \mathbb{P}^{\ell-1}(K)^3$ and $\widetilde{s} \in \widetilde{\mathbb{P}}^{\ell-1}(K)$.

Next, we assign to each face $f \in \mathcal{F}_h$ a unit normal $\mathbf{n}_f$. Then there is a unique element $K \in \mathcal{T}_h$ such that $f \subset \partial K$ and f is the image of the corresponding reference face $\widehat{f}$ on $\widehat{K}$ under the elemental mapping F_K, and such that $\mathbf{n}_f = B_K^{-T}\widehat{\mathbf{n}}_{\widehat{f}}/|B_K^{-T}\widehat{\mathbf{n}}_{\widehat{f}}|$, where $\widehat{\mathbf{n}}_{\widehat{f}}$ is the outward unit normal to $\widehat{f}$; cf. [11, Equation (5.21)]. We set

$$\mathbb{D}^\ell(f) = \{\, \mathbf{q}|_f \,:\, \mathbf{q}\circ F_K = B_K\widehat{\mathbf{q}},\ \mathbf{q}\in\mathbb{D}^\ell(\widehat{K}),\ \widehat{\mathbf{q}}\cdot\widehat{\mathbf{n}}_{\widehat{f}} = 0\,\}.$$

In local coordinates $\mathbf{x}$ on the face f, a function $\mathbf{q}|_f \in \mathbb{D}^\ell(f)$ is given by $\mathbf{q}|_f(\mathbf{x}) = \mathbf{r}(\mathbf{x}) + \widetilde{s}(\mathbf{x})\,\mathbf{x}$, where $\mathbf{r}\in\mathbb{P}^{\ell-1}(f)^2$ and $\widetilde{s}\in\widetilde{\mathbb{P}}^{\ell-1}(f)$. Notice that $\mathbf{q}|_f$ is tangential to f.

Finally, we assign to each edge e a unit vector $\mathbf{t}_e$ in the direction of e, and denote by $\mathbb{P}^\ell(e)$ the polynomials of degree ℓ on the edge e.

Step 2 (Moments for Nédélec's elements of the second type). We introduce a basis of $\mathbb{P}^\ell(K)^3$ that is based on the moments that define Nédélec's second family of elements introduced in [14]. Following [11], we use the following moments that are identical on K and $\widehat{K}$, up to sign changes, under the transformation $\mathbf{v}\circ F_K = B_K^{-T}\widehat{\mathbf{v}}$ (this can be easily seen as in [11, Lemma 5.34 and Section 8]).

For an edge e, let $\{q_e^i\}_{i=1}^{N_e}$ denote a basis of $\mathbb{P}^\ell(e)$. Similarly, let $\{\mathbf{q}_f^i\}_{i=1}^{N_f}$ be a basis of $\mathbb{D}^{\ell-1}(f)$ for a face f, and $\{\mathbf{q}_K^i\}_{i=1}^{N_b}$ a basis of $\mathbb{D}^{\ell-2}(K)$ for element K. Fix $K\in\mathcal{T}_h$ and let $\mathbf{v}\in\mathbb{P}^\ell(K)^3$. We introduce the following moments:

$$\begin{aligned}
M_K^e(\mathbf{v}) &= \left\{ \int_e (\mathbf{v}\cdot\mathbf{t}_e) q_e^i\, ds : i = 1,\ldots,N_e \right\}, &&\text{for any edge } e \text{ of } K,\\
M_K^f(\mathbf{v}) &= \left\{ \frac{1}{\mathrm{area}(f)}\int_f \mathbf{v}\cdot\mathbf{q}_f^i\, ds : i = 1,\ldots,N_f \right\}, &&\text{for any face } f \text{ of } K,\\
M_K^b(\mathbf{v}) &= \left\{ \int_K \mathbf{v}\cdot\mathbf{q}_K^i\, d\mathbf{x} : i = 1,\ldots,N_b \right\}.
\end{aligned}$$

It is well-known that the above moments uniquely define the polynomial $\mathbf{v}\in\mathbb{P}^\ell(K)^3$; see [14, 11]. For a face f of K, the tangential trace $\mathbf{n}_f\times\mathbf{v}$ is uniquely determined by the moments M_K^f and the moments $\{M_K^e\}_{e\in\mathcal{E}(f)}$, where $\mathcal{E}(f)$ is the set of the edges of f; see [14, Section 3.1] or [11, Lemma 8.11]. Hence, any $\mathbf{v}\in\mathbb{P}^\ell(K)^3$ can be written in the form

$$\mathbf{v} = \sum_{e\in\mathcal{E}(K)}\sum_{i=1}^{N_e} v_{K,e}^i \boldsymbol{\varphi}_{K,e}^i + \sum_{f\in\mathcal{F}(K)}\sum_{i=1}^{N_f} v_{K,f}^i \boldsymbol{\varphi}_{K,f}^i + \sum_{i=1}^{N_b} v_{K,b}^i \boldsymbol{\varphi}_{K,b}^i. \qquad (24)$$

Here, we use $\mathcal{E}(K)$ and $\mathcal{F}(K)$ to denote the sets of edges and faces of K, respectively. The functions $\{\boldsymbol{\varphi}_{K,e}^i\}$, $\{\boldsymbol{\varphi}_{K,f}^i\}$, and $\{\boldsymbol{\varphi}_{K,b}^i\}$ are Lagrange basis functions on $\mathbb{P}^\ell(K)^3$ with respect to the moments given above.

Step 3 (Bound of the elemental $H(\mathrm{curl})$–norm). Let $\mathbf{v}\in\mathbb{P}^\ell(K)^3$ be represented as in (24). We prove the following elemental bound on the

$H(\text{curl})$–norm in terms of the moments in Step 2: there exists a positive constant C, independent of the mesh size, such that

$$\|\mathbf{v}\|_{0,K}^2 + \|\nabla\times\mathbf{v}\|_{0,K}^2 \le Ch_K^{-1}\left[\sum_{e\in\mathcal{E}(K)}\sum_{i=1}^{N_e}(v_{K,e}^i)^2 + \sum_{f\in\mathcal{F}(K)}\sum_{i=1}^{N_f}(v_{K,f}^i)^2 + \sum_{i=1}^{N_b}(v_{K,b}^i)^2\right]. \quad (25)$$

On the reference element, this follows from the representation (24) and the Cauchy-Schwarz inequality. On a general element K, we note that since the transformation $\mathbf{v}\circ F_K = B_K^{-T}\hat{\mathbf{v}}$ preserves the moments in Step 2, and that

$$\|\mathbf{v}\|_{0,K}^2 \le Ch_K\|\hat{\mathbf{v}}\|_{0,K}^2, \qquad \|\nabla\times\mathbf{v}\|_{0,K}^2 \le Ch_K^{-1}\|\widehat{\nabla}\times\hat{\mathbf{v}}\|_{0,K}^2,$$

with a constant independent of the mesh size (see, e.g., [1, Lemma 5.2]), the bound in (25) is obtained.

Step 4 (Bound of the tangential jumps). Let f be an interior face shared by two elements K_1 and K_2. Denote by $\mathcal{E}(f)$ the edges of f. Let $\mathbf{v}_1 \in \mathbb{P}^\ell(K_1)^3$ and $\mathbf{v}_2 \in \mathbb{P}^\ell(K_2)^3$. We prove that, using the representation in (24), there exist positive constants C_1 and C_2, independent of the mesh size, such that

$$\int_f |\mathbf{n}_f\times(\mathbf{v}_1-\mathbf{v}_2)|^2 ds \le C_1\left[\sum_{i=1}^{N_f}(v_{K_1,f}^i - v_{K_2,f}^i)^2 + \sum_{e\in\mathcal{E}(f)}\sum_{i=1}^{N_e}(v_{K_1,e}^i - v_{K_2,e}^i)^2\right],$$

and

$$\left[\sum_{i=1}^{N_f}(v_{K_1,f}^i - v_{K_2,f}^i)^2 + \sum_{e\in\mathcal{E}(f)}\sum_{i=1}^{N_e}(v_{K_1,e}^i - v_{K_2,e}^i)^2\right] \le C_2\int_f |\mathbf{n}_f\times(\mathbf{v}_1-\mathbf{v}_2)|^2\, ds. \quad (26)$$

To see this, we first consider the case where K_1 and K_2 are of reference size. Since the moments on f and on the edges $e\in\mathcal{E}(f)$ uniquely determine the jump $\mathbf{n}_f\times(\mathbf{v}_1-\mathbf{v}_2)$, the claim follows from the equivalence of norms in finite dimensional spaces. For general elements K_1 and K_2, the claim is obtained from a scaling argument taking into account that the transformation $\mathbf{v}\circ F_K = B_K^{-T}\hat{\mathbf{v}}$ preserves tangential components and the moments in Step 2, modulo sign changes.

The analogous bound holds on the boundary. Let K be the element containing the boundary face f and $\mathbf{v}\in\mathbb{P}^\ell(K)^3$. Using the representation in (24), there exist positive constants C_1 and C_2, independent of the mesh size, such that

$$\int_f |\mathbf{n}_f \times \mathbf{v}|^2\, ds \le C_1 \left[\sum_{i=1}^{N_f} (v_{K,f}^i)^2 + \sum_{e\in\mathcal{E}(f)} \sum_{i=1}^{N_e} (v_{K,e}^i)^2 \right],$$

and

$$\left[\sum_{i=1}^{N_f} (v_{K,f}^i)^2 + \sum_{e\in\mathcal{E}(f)} \sum_{i=1}^{N_e} (v_{K,e}^i)^2 \right] \le C_2 \int_f |\mathbf{n}_f \times \mathbf{v}|^2\, ds.$$

Step 5 (Approximation property). For $\mathbf{v} \in \mathbf{V}_h$, we have

$$\inf_{\overline{\mathbf{v}}\in\mathbf{V}_h^c} \left[\|\varepsilon^{\frac{1}{2}}(\mathbf{v}-\overline{\mathbf{v}})\|_{0,\Omega}^2 + \|\mu^{-\frac{1}{2}}\nabla\times(\mathbf{v}-\overline{\mathbf{v}})\|_{0,\Omega}^2 \right] \le C\|\mathtt{m}^{-1}\mathtt{h}^{-1}|[\![\mathbf{v}]\!]_T|\|_{\mathcal{F}_h}^2, \tag{27}$$

with a positive constant C, independent of the mesh size.

To prove (27), let $\{v_{K,e}^i\}$, $\{v_{K,f}^i\}$ and $\{v_{K,b}^i\}$ denote the moments of $\mathbf{v}$, according to (24). Denote by $N(e)$ the set of all elements that share the edge e, and by $N(f)$ the set of all elements that share the face f. The cardinality of these sets are denoted by $|N(e)|$ and $|N(f)|$, respectively. Due to the shape-regularity of the meshes $\mathcal{T}_h$, we have that $1 \le |N(e)| \le N$, uniformly in the mesh size. Furthermore, $1 \le |N(f)| \le 2$. Let $\overline{\mathbf{v}} \in \mathbf{V}_h^c$ be the unique function whose edge moments are

$$\overline{v}_{K,e}^i = \begin{cases} \frac{1}{|N(e)|}\sum_{K'\in N(e)} v_{K',e}^i & \text{if } e \in \mathcal{E}_h^{\mathcal{I}}, \\ 0 & \text{if } e \in \mathcal{E}_h^{\mathcal{B}}, \end{cases}$$

$i = 1, \ldots, N_e$, whose face moments are

$$\overline{v}_{K,f}^i = \begin{cases} \frac{1}{|N(f)|}\sum_{K'\in N(f)} v_{K',f}^i & \text{if } f \in \mathcal{F}_h^{\mathcal{I}}, \\ 0 & \text{if } f \in \mathcal{F}_h^{\mathcal{B}}, \end{cases}$$

$i = 1, \ldots, N_f$, and whose remaining moments are

$$\overline{v}_{K,b}^i = v_{K,b}^i, \qquad i = 1, \ldots, N_b.$$

Obviously, the function $\overline{\mathbf{v}}$ defined by the above moments belongs to $H_0(\mathrm{curl};\Omega)$.

From the bound in (25) in Step 3 and the assumption (2) on the coefficients, we have

$$\begin{aligned} &\|\varepsilon_K^{\frac{1}{2}}(\mathbf{v}-\overline{\mathbf{v}})\|_{0,K}^2 + \|\mu_K^{-\frac{1}{2}}\nabla\times(\mathbf{v}-\overline{\mathbf{v}})\|_{0,K}^2 \\ &\quad \le C\mu_K^{-1}h_K^{-1} \left[\sum_{e\in\mathcal{E}(K)} \sum_{i=1}^{N_e} (v_{K,e}^i - \overline{v}_{K,e}^i)^2 + \sum_{f\in\mathcal{F}(K)} \sum_{i=1}^{N_f} (v_{K,f}^i - \overline{v}_{K,f}^i)^2 \right]. \end{aligned}$$

Let e first be an interior edge in $\mathcal{E}(K)$ and denote by $\mathcal{F}(e)$ the faces sharing the edge e. For $f \in \mathcal{F}(e)$, we denote by K_f and K'_f the elements that share f. Employing the definition of $\overline{u}^i_{K,e}$, the Cauchy-Schwarz inequality, bound (26) from Step 4, and the shape-regularity assumption gives

$$\begin{aligned}
\sum_{i=1}^{N_e}(v^i_{K,e} - \overline{v}^i_{K,e})^2 \;&\leq\; C \sum_{K' \in N(e)} \sum_{i=1}^{N_e}(v^i_{K,e} - v^i_{K',e})^2 \\
&\leq\; C \sum_{f \in \mathcal{F}(e)} \sum_{i=1}^{N_e}(v^i_{K_f,e} - v^i_{K'_f,e})^2 \\
&\leq\; C \sum_{f \in \mathcal{F}(e)} \int_f |[\![\mathbf{v}]\!]_T|^2 \, ds.
\end{aligned}$$

An analogous result holds for a boundary edge e.

Similarly, for an interior face $f \in \mathcal{F}(K)$, we have

$$\sum_{i=1}^{N_f}(v^i_{K,f} - \overline{v}^i_{K,f})^2 \leq C \sum_{K' \in N(f)} \sum_{i=1}^{N_f}(v^i_{K,f} - v^i_{K',f})^2 \leq C \int_f |[\![\mathbf{v}]\!]_T|^2 \, ds,$$

where we have again used the bound (26) from Step 4. An analogous results holds for boundary faces.

Combining the above estimates yields

$$\begin{aligned}
&\|\varepsilon_K^{\frac{1}{2}}(\mathbf{v} - \overline{\mathbf{v}})\|^2_{0,K} + \|\mu_K^{-\frac{1}{2}} \nabla \times (\mathbf{v} - \overline{\mathbf{v}})\|^2_{0,K} \\
&\quad \leq C \mu_K^{-1} h_K^{-1} \left[\sum_{e \in \mathcal{E}(K)} \sum_{f \in \mathcal{F}(e)} \int_f |[\![\mathbf{v}]\!]_T|^2 \, ds + \sum_{f \in \mathcal{F}(K)} \int_f |[\![\mathbf{v}]\!]_T|^2 \, ds \right].
\end{aligned}$$

Summing over all elements, taking into account the shape-regularity of the mesh and the definition of $\mathtt{m}$, proves (27).

Step 6 (Conclusion). We are now ready to prove (8). First, we note that the inequality on the right-hand side of (8) is trivial. To prove the left-hand side bound, we let $\mathbf{P}_h : \mathbf{V}_h \to \mathbf{V}_h^\perp$ denote the $\mathbf{V}(h)$–orthogonal projection. For $\mathbf{v} \in \mathbf{V}_h$, we have

$$\|\mathbf{P}_h \mathbf{v}\|_{\mathbf{V}(h)} = \inf_{\overline{\mathbf{v}} \in \mathbf{V}_h^c} \|\mathbf{v} - \overline{\mathbf{v}}\|_{\mathbf{V}(h)} \leq C \|\mathbf{P}_h \mathbf{v}\|_{\mathbf{V}_h^\perp}.$$

Here, we have used properties of orthogonal projections, the approximation result (27) from Step 5, the fact that $[\![\mathbf{v}]\!]_T = [\![\mathbf{P}_h \mathbf{v}]\!]_T$, and the definition of the norm $\|\cdot\|_{\mathbf{V}_h^\perp}$. Since $\mathbf{P}_h$ is surjective, this completes the proof of (8) in Theorem 2.

References

1. A. Alonso and A. Valli. An optimal domain decomposition preconditioner for low-frequency time-harmonic Maxwell equations. *Math. Comp.*, 68:607–631, 1999.
2. D.N. Arnold, F. Brezzi, B. Cockburn, and L.D. Marini. Unified analysis of discontinuous Galerkin methods for elliptic problems. *SIAM J. Numer. Anal.*, 39:1749–1779, 2001.
3. F. Brezzi and M. Fortin. Mixed and hybrid finite element methods. In *Springer Series in Computational Mathematics*, volume 15. Springer–Verlag, New York, 1991.
4. F. Brezzi and M. Fortin. A minimal stabilisation procedure for mixed finite element methods. *Numer. Math.*, 89:457–491, 2001.
5. L. Demkowicz and L. Vardapetyan. Modeling of electromagnetic absorption/scattering problems using *hp*–adaptive finite elements. *Comput. Methods Appl. Mech. Engrg.*, 152:103–124, 1998.
6. R. Hiptmair. Finite elements in computational electromagnetism. *Acta Numerica*, pages 237–339, 2003.
7. P. Houston, I. Perugia, and D. Schötzau. Nonconforming mixed finite element approximations to time-harmonic eddy current problems. In *Proceedings of the 14th COMPUMAG Conference on the Computation of Electromagnetic Fields*, Saratoga Springs, NY, USA, July 13-17, 2003.
8. P. Houston, I. Perugia, and D. Schötzau. Mixed discontinuous Galerkin approximation of the Maxwell operator. Technical Report 02-16, University of Basel, Department of Mathematics, 2002.
9. P. Houston, I. Perugia, and D. Schötzau. *hp*-DGFEM for Maxwell's equations. In F. Brezzi, A. Buffa, S. Corsaro, and A. Murli, editors, *Numerical Mathematics and Advanced Applications ENUMATH 2001*, pages 785–794. Springer-Verlag, 2003.
10. O.A. Karakashian and F. Pascal. A posteriori error estimation for a discontinuous Galerkin approximation of second order elliptic problems. Technical report, University of Tennessee, Department of Mathematics, 2003. Report can be retrieved from: `http://www.math.utk.edu/~ohannes/papers.html`. To appear in SIAM J. Numer. Anal.
11. P. Monk. *Finite element methods for Maxwell's equations.* Oxford University Press, New York, 2003.
12. J.C. Nédélec. Mixed finite elements in $\mathbb{R}^3$. *Numer. Math.*, 35:315–341, 1980.
13. J.C. Nédélec. Éléments finis mixtes incompressibles pour l'équation de Stokes dans $\mathbb{R}^3$. *Numer. Math.*, 39:97–112, 1982.
14. J.C. Nédélec. A new family of mixed finite elements in $\mathbb{R}^3$. *Numer. Math.*, 50:57–81, 1986.
15. I. Perugia and D. Schötzau. The *hp*-local discontinuous Galerkin method for low-frequency time-harmonic Maxwell equations. *Math. Comp.*, 72:1179–1214, 2003.
16. I. Perugia, D. Schötzau, and P. Monk. Stabilized interior penalty methods for the time-harmonic Maxwell equations. *Comput. Methods Appl. Mech. Engrg.*, 191:4675–4697, 2002.
17. L. Vardapetyan and L. Demkowicz. *hp*-adaptive finite elements in electromagnetics. *Comput. Methods Appl. Mech. Engrg.*, 169:331–344, 1999.